1-1-2006

# Water assisted laser cutting of brittle materials

Christopher Daniel Barnes
*Iowa State University*

# Water assisted laser cutting of brittle materials

by

**Christopher Daniel Barnes**

A thesis submitted to the graduate faculty

in partial fulfillment of the requirements for the degree of

MASTER OF SCIENCE

Major: Mechanical Engineering

Program of Study Committee:
Pal Molian, Co-major Professor
Pranav Shrotriya, Co-major Professor
Frank Peters

Iowa State University
Ames, IA
2006

Graduate College
Iowa State University

This is to certify that the master's thesis of

Christopher Daniel Barnes

Has met the thesis requirements of Iowa State University

Signatures have been redacted for privacy

## Table of Contents

# Chapter 1: General Introduction

## 1.1 Cutting of Brittle Materials

Due to their outstanding physical and chemical properties, ceramics are increasingly being used in many applications. However, their inherent brittleness often leads to costly difficulties in processing and machining, particularly when shaping or finishing operations are involved. Diamond drilling, sand blasting, sawing, electric discharge and ultrasonic machining of brittle materials have been widely regarded as adequate traditional processes to machine concrete, stone, glass, silicon and alumina. Although these processes have become widely popular to machine brittle materials, these methods are inherently plagued with problems including: 1) the formation of large amounts of debris, 2) expense, 3) the build up of residual stresses, 4) the need of skilled labor, 5) time-consuming 6) the need for replacement tooling 7) difficulty in contour shaping of materials [1-3].

Since some of the traditional methods of cutting and machining brittle materials have certain disadvantages; nontraditional methods of machining brittle materials have also been explored. Among these processes three particular ones have been widely accepted. Water-jet, abrasive water-jet and laser cutting have been common practice in cutting brittle materials. Water-jet and abrasive water-jet technologies have been proven extensively for cutting and drilling concrete, rock and minerals [4-7]. Water-jet uses only high pressure water (up to 70,000 psi), while abrasive water-jet uses garnet abrasives along with high pressure water. There is a maximum water pressure for water-jet depending on the material's compressive strength, permeability, moisture content, crystalline structure and other particular characteristics. If a particular material has problems with extremely high

pressures applied to it, abrasive water-jet machining can be used. Since this process uses abrasive materials in the water-jet stream, less pressure is needed. Also, abrasive water-jet machining is capable of cutting thicker materials with out heating or vibrating the work piece. Because these processes use high pressure water as the cutting tool, high power pumps and limited water flow capacity can become inherent problems while using this mode of cutting.

Laser cutting has recently become a prominent way to cut and engrave materials. This process is not used as frequently in construction environments, never the less it is widely used in industrial settings. Laser cutting can be used for very precise cutting and engraving. Although this type of method is non-contact in nature, it is not used for cutting due to the nature of the material removal. Since laser cutting is non-contact in nature, material must be removed by evaporation or melting. This mode of material removal inherently uses very high powers and can lead to thermal stresses which can cause unwanted fracturing.

With the use of a hybrid system that uses a laser and water-jet (LWJ) to thermally fracture materials, many of the problems stated above can be avoided. Using the water as a quenching catalyst and material removal process, this process would be able to efficiently use the inherent transient heat build up in the material while not have the primary problem of material removal.

### 1.2 Concept of Hybrid Laser Water/Jet Cutting

The underlying hypothesis of the LWJ process is that elements of laser and water-jet machining can be synergistically combined such that material removal is accomplished by thermal-shock fracturing of material into fine fragments rather than energy-intensive erosive

wear or melting and subsequent evaporation. The LWJ process consists of a low-power laser for precise heating of a small processing zone on the work piece.

The laser heating will create temperature gradient in a zone approximately equal to thermal diffusion depth and rapid quenching of the zone by a low-pressure water-jet will cause development of thermal stresses that fracture this zone. The cycle of laser heating and water cooling will produce thermal shock, a phenomenon associated with rapid changes in the temperature generating internal thermal stresses and causing the brittle materials — that exhibit low thermal conductivity and tensile strength, and high thermal expansion and modulus — to fracture. Rapid cooling rather than rapid heating will inflict most of thermal shock fracture since the induced surface stresses are tensile in nature during rapid cooling. The fractured debris will be removed through the kinetic energy of water-jet. In this way, we can avoid the formation of liquid and gaseous phases, making the process more energy efficient and free from hazardous emission. The LWJ process meets the challenges of energy and environmental consciousness in the machining of brittle materials.

During thermal shock fracture due to rapid cooling, pre-existing flaws in the laser heated zone may grow into three possible crack configurations — edge crack or meridian crack towards center of plate, channeling crack and spalling crack. The edge crack is the ideal configuration for manufacturing, because of the direction in which it propagates through a material. Channeling cracks that propagate along the path of laser beam are also beneficial but channeling crack that deviate from laser path and spalling cracks will propagate away from processing zone and lead to damage of the machined surfaces. Figure 1 illustrates these types of cracks.

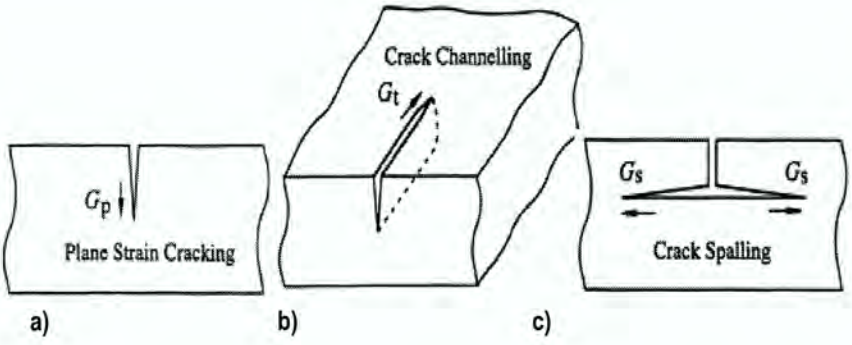


**Figure 1: Possible crack configurations: a) edge crack or meridian crack; b) channeling crack; c) spalling crack**

In the current work, the fracture characteristics and cut quality of single strips of glass, silicon, concrete and alumina by LWJ were determined and analyzed in order to investigate the material removal mechanism and crack formation associated with thermal shock fracture.

### 1.3 Literature Review

Elperin et al. analyzes a laser method that separates wafers manufactured from ceramic materials based on double thermal shock. In their study the authors hypothesis that surface cracks could be formed on wafers so that they could be separated more easily. In their study the wafer was heated using a $CO_2$ laser and then immediately cooled by an air-water spray. The experimental data was used to develop a model describing the method for thermally splitting glass and glass-like materials. They concluded that it was possible to form surface cracks on wafers with the combined use of laser heating and cooling. They also found that it was possible to manipulate the crack so that it followed the laser heated area and was hence

"controlled" [8]. Tsai et al. supported these findings by coming to the conclusion that it is possible to thermally fracture materials, specifically alumina. In Tsia's study the author's performed all their experiments with a $CO_2$ laser. The authors hypothesized that controlled fracture of alumina was possible by using a $CO_2$ laser to heat up the material while air was used for the cooling process. In these experiments .635mm thick alumina was cut with a 30 watt laser while the laser spot size was varied. Observations were made based on cracks that appeared due to thermal stresses in the material. The authors came to the conclusion that there are three stages to thermally cracking alumina: 1) the initiation of the fracture occurs due to tensile stress at the edge of the specimen, 2) the stable growth stage, when the stress near the laser spot behaves highly compressive, after the laser passing, the plastic compressive stress will be relaxed and then induce a residual tensile stress near the upper surface, 3) the final stage is unstable fracture, the stress near the crack tip is totally a tensile stress through the thickness direction, so that the crack will extend unstably [9]. Although the Tsia's study does not use water or some other catalyst for thermally shocking the alumina, the results are quite interesting and confirm this author's findings that using air as a cooling agent can cause uncontrollable cracking.

Zhou et al. studies thermal shock of metal matrix composites induced by a laser, specifically SiC. The study also uses a finite element model to simulate the temperature and thus the stress field that is created due to thermal gradients in the materials. The goal of their study is to examine the thermal stresses and temperature fields created by a laser and the study the possibility if it could be modeled with FEA. The authors used a Nd:glass pulsed laser and varied the energy input from 1J to 40J. Although it was found that the materials could be thermally cracked with the laser, the interesting insight is that the FEA

model was successful at predicting cracks in the materials. The FEA numerical analysis was based off of the thermal gradients found in the materials during experimentation. Based off of the temperature the correct stresses could be calculated and fracturing criteria could be found [10].

### 1.4 Research Objectives

Brittle materials (granite, concrete, silicon, glass and alumina) are difficult to machine economically and efficiently using traditional as well as contemporary non-traditional processes. Also, cutting these types of materials with just a laser consumes large amounts of power and has material removal problems; due to the fact that laser uses evaporation as a means to remove material. The goal of this research is to investigate the thermal shock and fracture mode of material removal in a hybrid laser/water-jet (LWJ) manufacturing process for brittle materials. Several different brittle materials (glass, silicon, concrete and alumina) will be cut using a LWJ and then compared to samples that are cut by the laser only. These samples will be looked at for overall quality, depth of cut, crack propagation and power uses. Also, a numerical program will be studied and developed using an FEA (Abaqus) package. This program will be used to determine temperatures, stresses, power requirements and material properties. With these experimental studies and the numerical program, it is believed that they will sufficiently help determine the criteria and characteristics of thermally shock fracturing of brittle materials.

## 1.5 Thesis Outline

The thesis consists of a brief chapter that will help give a general introduction and concept of using a LWJ, which will talk about the need and possible advantages of using a hybrid system.

Chapter 2 reveals and discusses the experimental results using the LWJ on glass, silicon and concrete. These results are compared to samples of the same materials cut with the laser alone. Details of the experimental technique will be discusses along with an additional experiment that was run to define certain criteria needed to exhibit uncontrolled cracking in glass. It will also discuss the advantages of using a hybrid system instead of traditional and non-traditional methods.

Chapter 3 will describe the results of cutting alumina by thermally fracturing it using a laser and water along with developing a numerical model to help in predicting fracturing in the sample. The chapter will touch briefly on uses of alumina in industry and the advantages a thermally fracturing hybrid system has. The experimental procedure is discussed in depth and illustrations of the data collecting are shown. Specific criteria of energy inputs and cooling rate for controlled cracking will be analyzed. The FEA program will be run to simulate certain parameters and the temperature and stress contours will be developed and discussed. Finally, conclusions about the cutting of alumina by using thermal fracturing will be drawn, based off of the ability to control the cracking.

Chapter 4 will talk about overall conclusions that can be drawn from the data that was collected and analyzed. Also, future work and improvements will be discussed.

## 1.6 References

1) Sheppard, L.M.., "Machining of Advanced Ceramics", Advanced Materials and Processes, ASM, Vol. 12, pg. 40, 1987.

2) B.E. Brath, "$CO_2$ Laser Cutting of Ceramic Tile", Beng. Dissertation, Heriot-Watt Univeristy, Edinburgh, UK, 1994.

3) H.K. Tönshoff, B. Denkena, H.H. Apmann and J. Asche, (2003), "Diamond Tools in Stone and Civil Engineering Industry - Cutting Principles, Wear and Applications," Machining of Natural and Stone Materials, Trans Tech Publications, p.103.

4) 2. X.H. Li, Y, Y. Liao, X.Y. Lei, et al. "Jiao Numerically Controlled Water Cutter and its Applications in the Machining of Natural Rock Materials", Machining of Natural and Stone Materials. Pg. 274, Trans Tech Publication, 2003.

5) LAI International. Home Page. 15 Feb. http://www.abrasivewaterjet.com/lai/tech.html

6) M. Hashish, "Experimental Studies of Cutting with Abrasive Waterjets", Proceedings of the 2nd U.S. Water Jet Conference, WJTA, 1983, 402.

7) M. Hashish, W.V. Loscutoff and P. Reich, "Cutting with Abrasive Waterjets", Proceedings of the 2nd U.S. Water Jet Conference, WJTA, 1983, 417.

8) Elperin, T., Kornilov, A., and Rudin, G., "Formation of Surface Micro-cracking for Separation of Nonmetallic Wafers Into Chips", Journal of Electronic Packaging, Vol. 122, pgs. 317-322, December, 2000.

9) Tsai, Chwan-Huei, Liou, Chi-Sheng, "Fracture Mechanism of Laser Cutting With Controlled Fracture", Journal of Manufacturing Science and Engineering, ASME, Vol. 125, pgs. 519-528, August, 2003.

10) Zhou, Y.C., Long, S.G. and Y.W. Liu. "Thermal failure mechanism and failure threshold of SiC reinforced metal matrix composites induced by laser beam", Mechanics of Materials, Vol. 35. pgs. 1003-1020, 2003.

# Chapter 2: A Hybrid Laser/Water-Jet Cutting Process for Brittle Materials

A paper presented at the 34th NAMRC Conference in Marquette University

Christopher Barnes, Pranav Shrotriya and Pal Molian
Laboratory for Lasers, MEMS and Nanotechnology
Department of Mechanical Engineering
Iowa State University
Ames, IA 50011

**Keywords**

Laser, water-jet, cutting, brittle materials, synergy

## 2.1 Abstract

The synergistic effects of coupling laser and water-jet on the material removal mechanism and energy efficiency were investigated in cutting of glass, silicon and concrete. A hybrid laser/water-jet (LWJ) manufacturing process was utilized to machine samples at low pressures of water-jet (<100 psi) and low powers (<500 W) of $CO_2$ laser and results were compared to the samples that were cut with just laser alone. The water-jet enabled the laser beam to cut the materials by thermal stress fracturing and washing away the debris from the kerf. It was found that glass and silicon acted very similar to each other and produced good quality cuts. However, the hybrid method had a relatively smaller effect on concrete. The proposed mechanism involves induction of compressive stresses during laser heating followed by a change in stress field to tension during water-jet cooling, leading to crack initiation and growth from the top to bottom surface. Due to the LWJ capability of removing material by thermally shock-induced fracture rather than energy-intensive erosive

wear (water-jet) or melting and subsequent evaporation (laser); it offers potential benefits such as reduced energy, increased cutting speed, improved accuracy and finish, and controlled depth and shape.

## 2.2 Introduction

In the last few decades, cutting and shaping of brittle materials such as concrete, stone, glass and granite has become a huge market. According to the International Association of Concrete Drillers and Sawers, the total world market for concrete cutting was approximately $9 billion in 2003. With the anticipated increase in market size, the industry is seeking better and more efficient methods of cutting brittle materials. Diamond drilling and sawing technology, developed using industrial diamond and cubic boron nitride materials, is widely regarded throughout industry as an adequate method for cutting and shaping granite, stone, concrete and tile [1]. Although this method is used extensively, the following drawbacks make this method less attractive: high cost of diamond tooling; need for skilled labor; environmental and safety problems; low speed; and low precision. In addition, contemporary trends —explosive growth in the number of components; movement towards small sizes in the microelectronics and nanotechnology fields; increasing use of brittle materials such as silicon and glass — require newer methods of machining that are less energy intensive and produce precise cuts. Consequently, non-traditional machining methods are considered, studied and assessed.

Non-traditional methods such as water-jet cutting, laser cutting, laser-microjet cutting and abrasive water-jet cutting are well recognized for cutting brittle materials. Water-jet cutting and abrasive water-jet cutting (pressures range from 7000 psi to 70,000 psi

depending on the type of brittle material) have already proven effective in cutting concrete and stone [2-4]. Laser cutting is a well established cutting method for plastics, woods and metals, yet there are few works reported on laser cutting of brittle materials [5, 6]. Although laser cutting is non-contact in nature it has problems with the mechanism of material removal, which involves evaporating, melting and blowing with a gas stream which is only possible with the use of very high-power lasers.

Laser-microjet cutting (LMJ) is a recent method that uses a 30-60 μm diameter water-jet as a waveguide and a pulsed fiber or Nd:YAG laser to focus the beam directly into the jet [7, 8]. The laser is guided by reflection of the air-water interface, similar to an optical fiber. The main applications of LMJ are cutting metal stents, stencils, silicon wafers, honeycombs, laminates, and sandwich structures that benefit semiconductor, electronic, medical, energy, and automotive industries. LMJ is limited to extreme thin sections and can therefore not be of practical use in cutting most brittle materials that are thicker in nature.

It is apparent that machining of brittle materials is a challenging task using traditional as well as contemporary non-traditional processes. Traditional machining methods are characterized by great loss of material as well as tool failure and it is hard to achieve the design requirements of high precision, complex shape and excellent surface integrity. Contemporary non-traditional processes suffer from: high-power requirements (lasers ~ 2-10 kW, water-jet ~ 40,000 psi pressure), energy inefficiency, hazardous fumes (laser), abrasive requirements (water-jet), slow machining rates (water-jet), wear of machinery components (water-jet), etc.

With the growing market for machining of brittle materials, it is imperative to examine new methods to shape and/or cut these materials. One such method is a hybrid laser and water-

jet apparatus (LWJ) that utilizes low power $CO_2$ laser and low pressure water-jet and capitalizes on the synergistic effects through thermal shock fracture of workpiece materials. A hybrid machining process is one in which either both of the constituent processes are directly involved in the material removal process or only one of the participating processes directly removes the material while the other assists in removal by changing the machining conditions in a positive way. The water-jet in this hybrid set up is designed to assist in creating thermal stress cracks and to aid in washing away of cracked material.

### 2.3 Concept of Laser/Water-Jet Cutting

The underlying hypothesis of the LWJ process is that elements of laser and water-jet machining can be synergistically combined such that material removal is accomplished by thermal-shock fracturing of material into fine fragments rather than energy-intensive erosive wear or melting and subsequent evaporation. The LWJ process (Figure 1) consists of a low-power laser for precise heating of a small processing zone on the work piece.

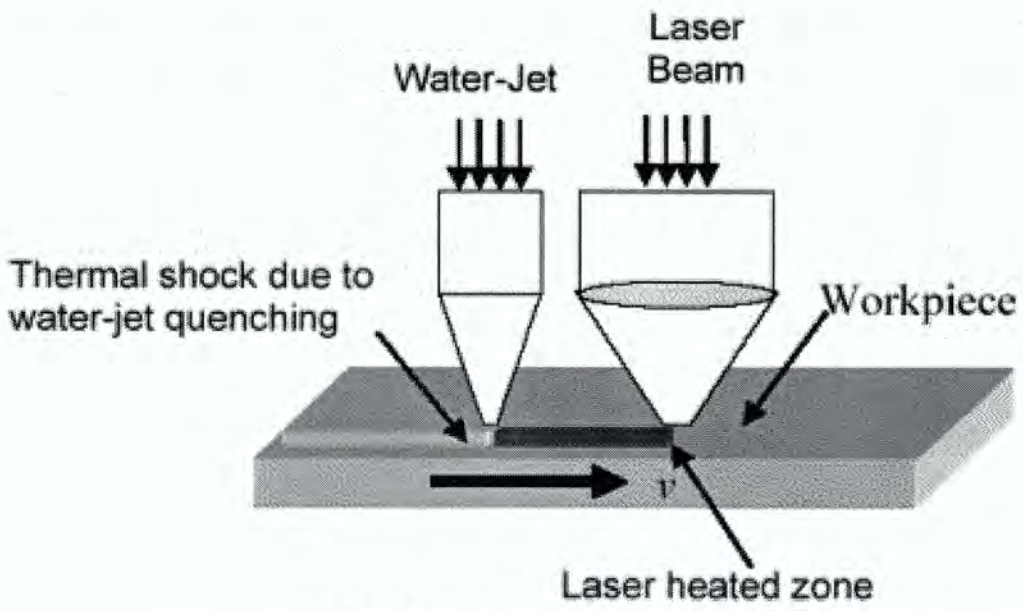


**Fig 1: Laser/Water Jet experimental set up.**

The laser heating will create temperature gradient in a zone approximately equal to thermal diffusion depth and rapid quenching of the zone by a low-pressure water-jet will cause development of thermal stresses that fracture this zone. The cycle of laser heating and water cooling will produce thermal shock, a phenomenon associated with rapid changes in the temperature generating internal thermal stresses and causing the brittle materials – that exhibit low thermal conductivity and tensile strength, and high thermal expansion and modulus – to fracture. Rapid cooling rather than rapid heating will inflict most of thermal shock fracture since the induced surface stresses are tensile in nature during rapid cooling. The fractured debris will be removed through the kinetic energy of water-jet. In this way, we can avoid the formation of liquid and gaseous phases, making the process more energy efficient and free from hazardous emission. The LWJ process meets the challenges of energy and environmental consciousness in the machining of brittle materials.

During thermal shock fracture due to rapid cooling, pre-existing flaws in the laser heated zone may grow into three possible crack configurations — edge crack or meridian crack towards center of plate, channeling crack and spalling crack — schematically represented in Figure 2. Clearly, the edge crack is the ideal configuration for manufacturing. Channeling cracks that propagate along the path of laser beam are also beneficial but channeling crack that deviate from laser path and spalling cracks will propagate away from processing zone and lead to damage of the machined surfaces.

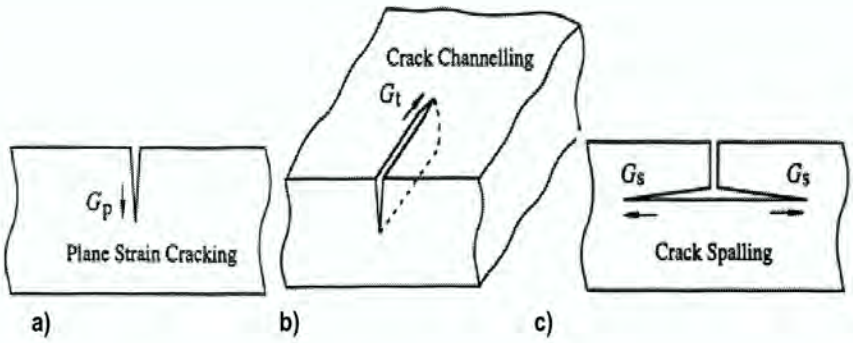


**Figure 2: Possible crack configurations: a) edge crack or meridian crack; b) channeling crack; c) spalling crack**

In the current work, the fracture characteristics and cut quality of single strips of glass, silicon and concrete by LWJ were determined and analyzed in order to investigate the material removal mechanism and crack formation associated with thermal shock fracture.

## 2.4 Experimental Procedure

A 1.5 kW continuous wave $CO_2$ laser with an *x-y* computer numerical controlled (CNC) positioning table was used for the cutting experiments. The materials used for machining experiments were silicon, glass and concrete. The specimens were set on the positioning table and the laser beam was focused with a 127 mm (5 in.) focal length lens directly on the specimen surface to a spot size of ~0.2 mm. The water-jet apparatus was mounted on the same *x-y* CNC table by adding a water pump and a recirculation water basin. A thin stream of water (approximately 0.3 gal/min and 60 psi) was pumped onto the specimen while being cut. In order to investigate the material removal mechanism, water-jet pressure was

maintained low such that laser heated zone is quenched but fractured material is not washed away.

### *2.4.1 Glass*

The glass specimens were microscopy slides with a size of 75 mm x 25 mm x 1 mm (2.99 in. x 0.91 in. x 0.04 in.). Laser power varying from 130 to 500 watts and feed rates ranging 4.23 mm/sec to 42.33 mm/sec (10 to 100 inch/min) were used to cut the single slide specimens. The depth of cut was measured, cracks were observed and process parameter window was established. The experiments were carried out with powers ranging from 170 to 390 watts with feed rates ranging from 12.7 mm/sec to 42.33 mm/sec (30 to 100 inch/min). The crack formation site and cut quality were characterized.

### *2.4.2 Silicon*

The silicon wafer used was a <100> single crystalline with dimensions of 100 mm (4 in.) diameter and 500 μm (0.02 in.) thick. A 130 nm thick film of oxide was grown on the silicon wafer to help reduce the reflectivity of the laser beam. The oxide was grown by placing the silicon wafer in an oven at 1000°C for 4 hours. In the cutting experiments, the laser power was varied from 130 to 500 watts while the feed rate was increased from 8.47 to 84.7 mm/sec ((20-200 inch/min) for both water-jet and non water-jet assisted samples. The samples that were not cut all the way through were mechanically broken and the cross-sections were examined, photographed and cut depths were measured on a computer using a image analysis software.

### *2.4.3 Concrete*

The concrete samples used in this study were prepared in Civil and Construction Engineering department of Iowa State by mixing limestone and silica sand in specific proportion with water. The cast samples were cut off from a 100 mm (4 in.) diameter "cylinder". Samples of different thicknesses (varying from 3 mm to 6.4 mm (0.12 in. to 0.25 in.)) were cut at laser powers from 500 to 1500 W and at feed rates between 8.7 mm/sec to 42.3 mm/sec (20-100 inch/min). The depth and width of cuts were measured. Experiments were also conducted with different initial temperatures of concrete. Some samples were presoaked in water for 24 hours and then frozen in a refrigerator while others were immersed in liquid nitrogen. All cuts were made 76 mm (3 in.) long, starting from the edge.

## 2.5 Results

The characteristics of all three materials cut by laser alone as well as by LWJ are presented below.

### *2.5.1 Glass Slides*

Power-feed rate plots for both laser alone and LWJ cutting are shown in Figure 3. The plots are divided into two zones: complete cutting (cut-through) and partial cutting (scribing). The cut-through mode in both cases is due to melting and evaporation mechanisms of material removal. Due to the presence of water, it takes more laser power for cutting the glass in LWJ. For example, it takes 280 W to cut through in LWJ as opposed to 120 W in just laser alone for a feed rate of 4.23 mm/sec (10 in/min). However, in the scribing mode, the laser-alone-cut causes material removal through evaporation/melting

while the LWJ causes material removal through thermal cracking, suggesting the potential of energy efficiency. Of course, the energy benefits are not realized in this case partly due to small thickness of the samples. It may be noted in Figure 3 that the process parameter window for scribing is much larger in LWJ than in laser alone.

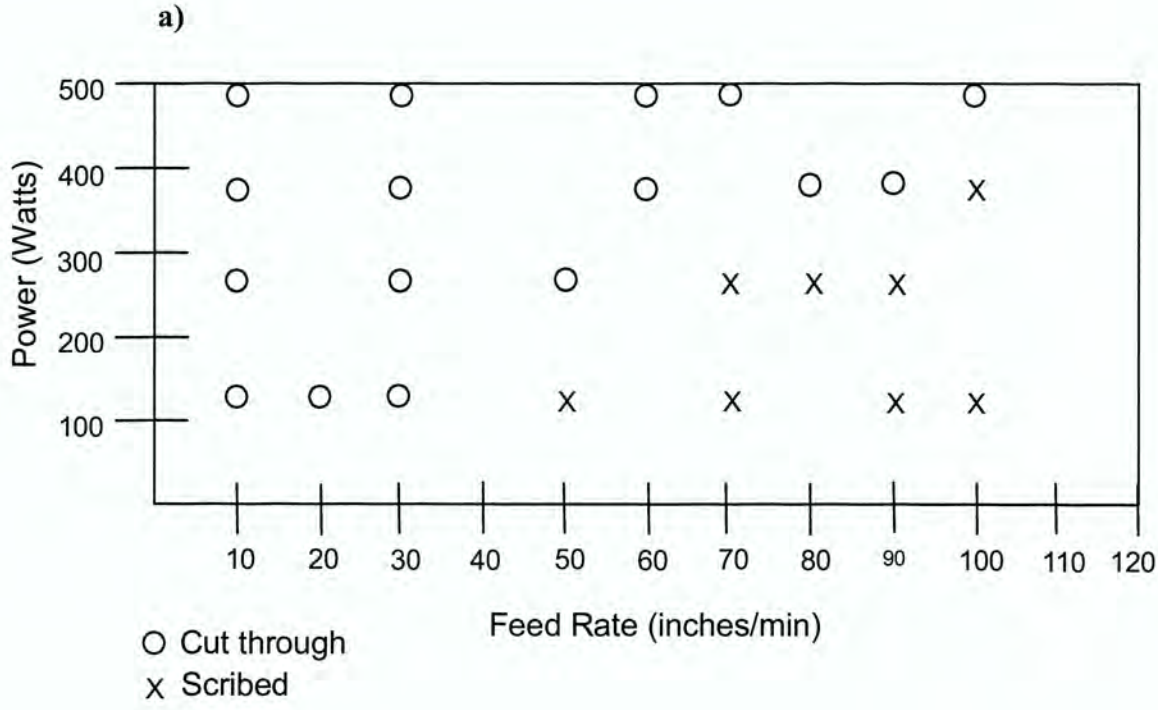

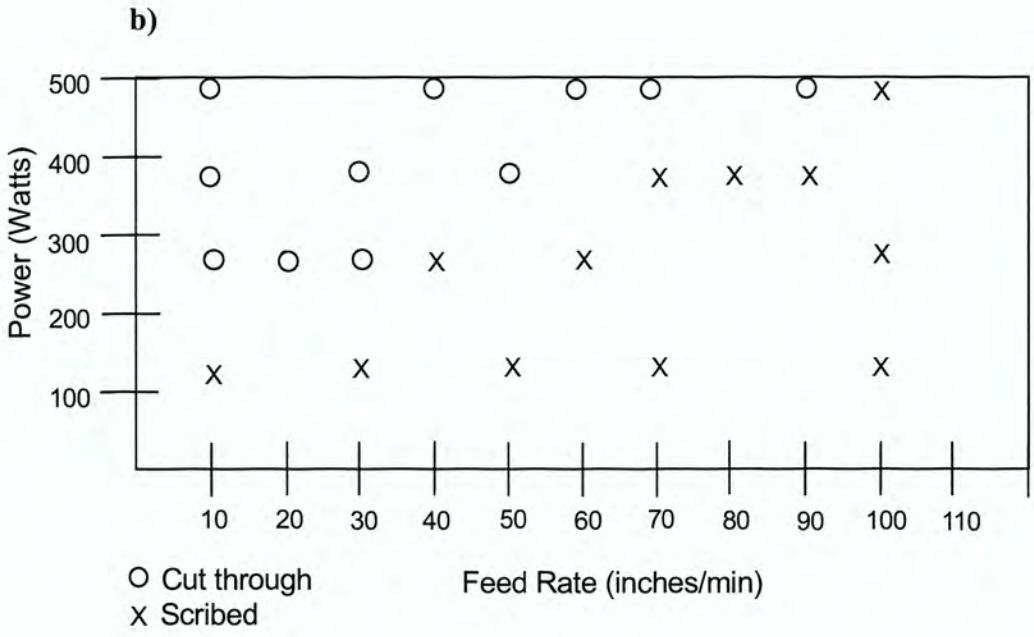


**Figure 3: (a) Plot of glass cutting with laser alone; (b) Plot of glass cutting with water-jet and laser.**

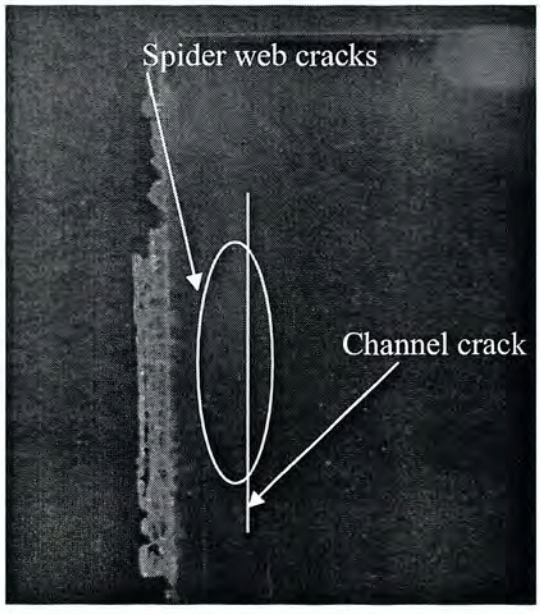


**Figure 4: Spider web and channel cracks in LWJ scribed glass.**

The LWJ scribed (thermally cracked) samples were much easier and cleaner to break than laser-alone-cut scribed (evaporated/melted) samples. In LWJ, multiple cracks with an approximate size of 0.5 mm (0.02 in) arranged in a spider-web configuration were formed in the cut zone (Figure 4). This spider web effect produced an area that was made up of very small fragments of glass, thus making it easier to break along the cut zone. Also, channel cracks started at the edge of the slide, where the laser beam had began, and then propagated along both sides of the cut zone. Some of the cracks propagated away from the side of the cut at approximately 45 degrees until they hit the edges of the glass slide.

### *2.5.2 Silicon*

The LWJ produced similar results in silicon to those of glass slides; however, the effects are more pronounced. A plot of laser power-feed rate is shown in Figure 5, where the top (solid) line represents the boundary between cut-through and scribing in LWJ while the

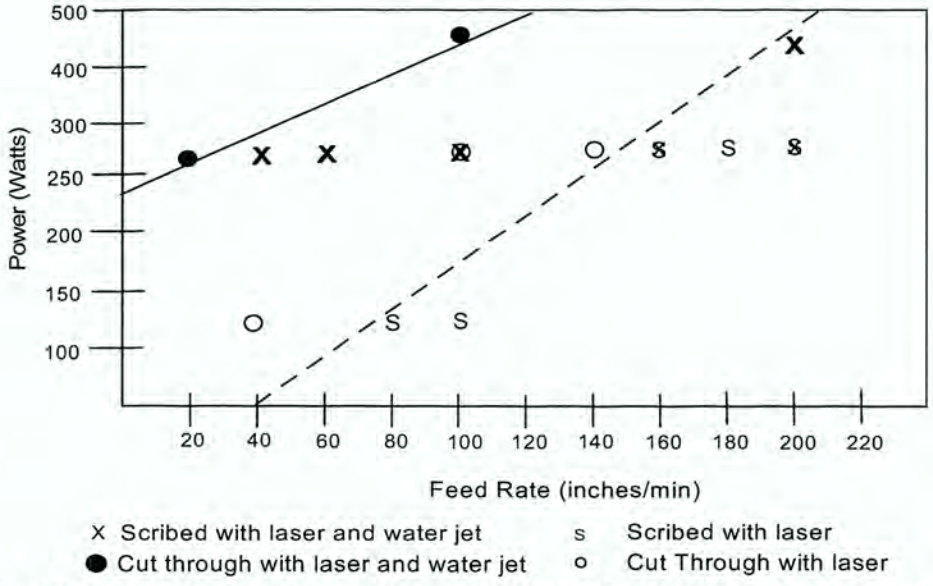


**Figure 5: Laser power-feed rate plot for cutting silicon with laser alone and LWJ.**

bottom (dashed) line represents the same in laser-alone. Although it takes more energy in LWJ (due to high power and slow speed) for scribing, thermal shock produced edge or meridian cracks that made it easier break the wafer along the scribe lines compared to wafers scribed by laser alone.

Figure 6a and b show the scanning electron micrographs of cross-sections of the silicon samples scribed (and later fractured by mechanical means) by LWJ and laser alone respectively. In both cases, a small distinct region near the top (heat affected zone, d) is an effect caused by the laser alone. Below the heat affected zone, is the fracture zone (j). It may be noted that the surface integrity of laser-alone-cut sample is inferior to the LWJ sample. In addition, surface roughness measurements indicate that the sample that was cut with the LWJ had a lower roughness than the sample that was cut with the laser, alone. The surface $R_a$ was measured using an atomic force microscope (AFM) were 9.42 nm and 80.88 nm at a 7.5 μm scale were found for the LWJ and the laser cut samples respectively. Also taken at a 7.5 μm scale, the $R_t$ values were 20.41 nm and 92.23 nm for the LWJ and laser cut samples respectively. The LWJ sample exhibited a considerably better quality because of the formation of edge cracks.

a)

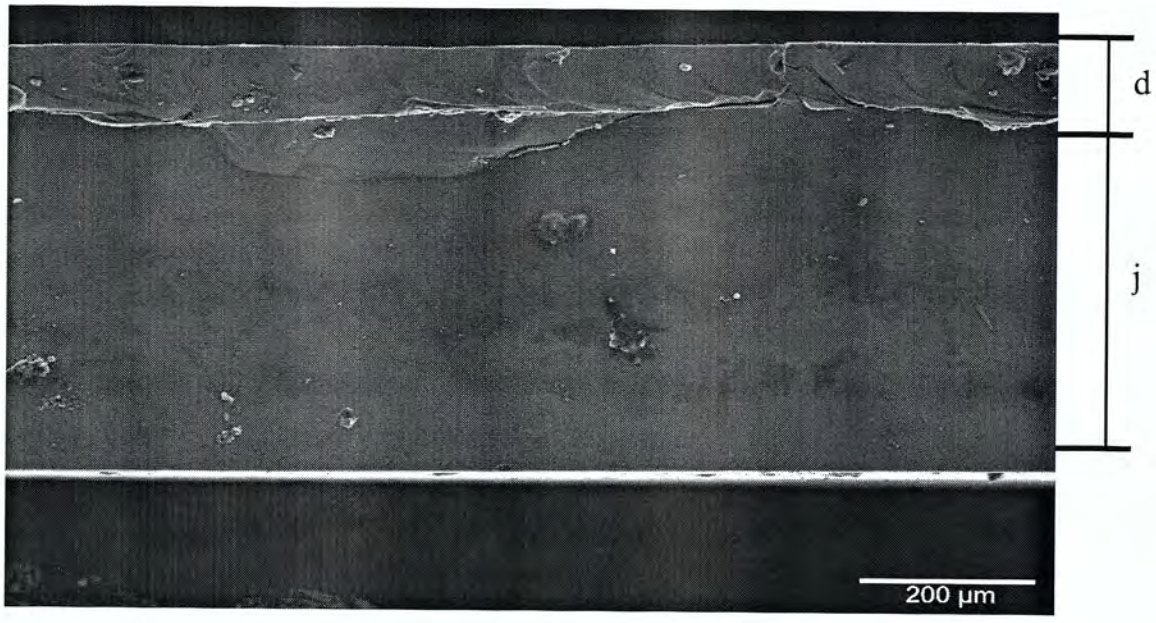


b)

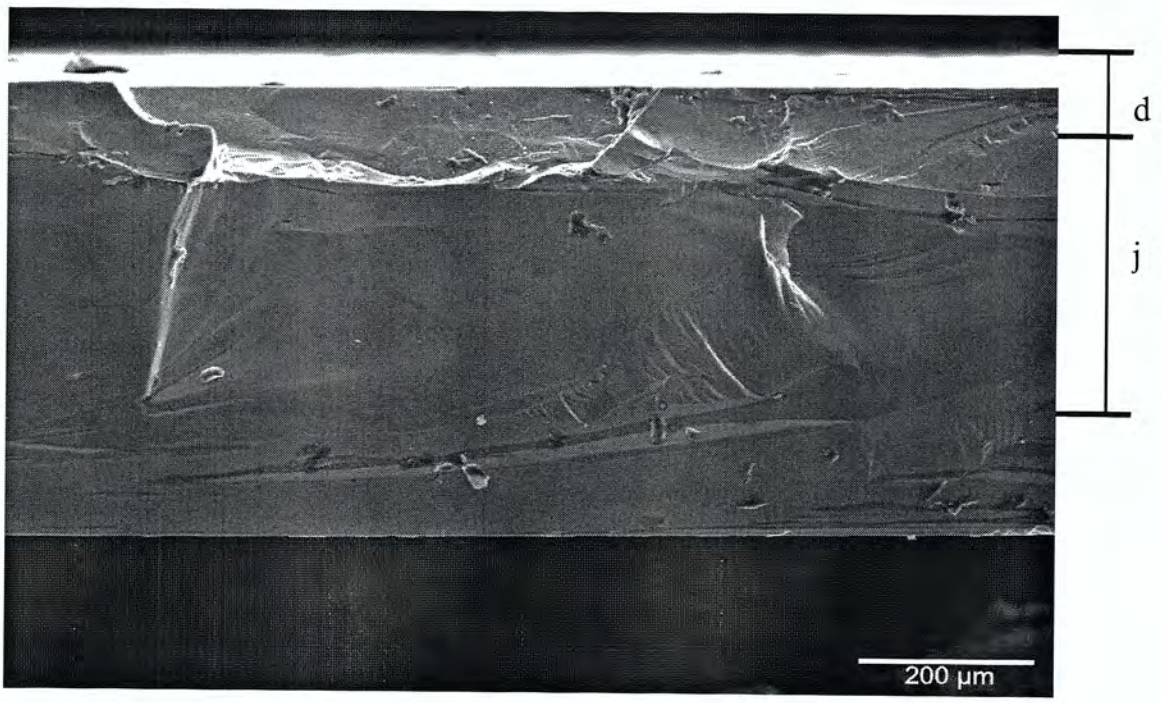


**Figure 6. Scanning electron micrographs of scribed and cut silicon: a) LWJ; b) Laser alone**

The 3-D plots of depth of cut as a function of power and feed rate for LWJ and laser-alone cuts are shown in Figure 7. Both plots show the expected result that deeper cuts are obtained with increased power and reduced feed rate. However, two interesting observations are: 1) the feed rate has a greater influence in laser-alone than in LWJ cutting; 2) the laser power effect is not linear in LWJ. Finally, these data provide that the energy efficiency is not significantly improved during scribing in LWJ compared to laser-alone although much lower forces are required to mechanically fracture the sample in case of LWJ.

**a)**

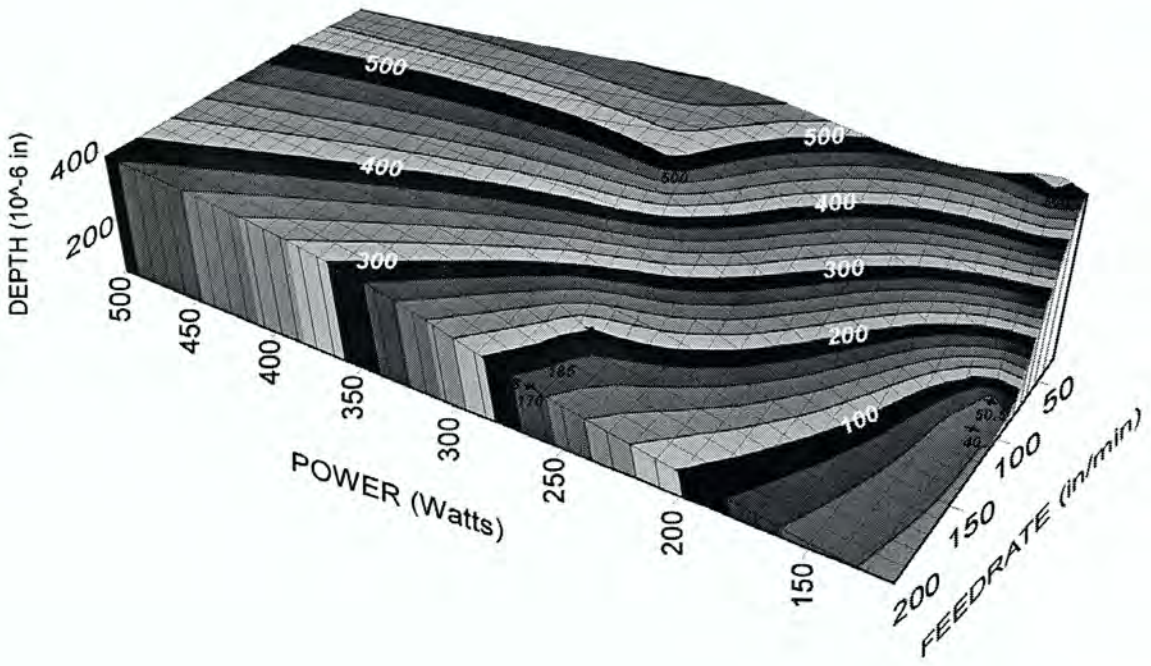

b)

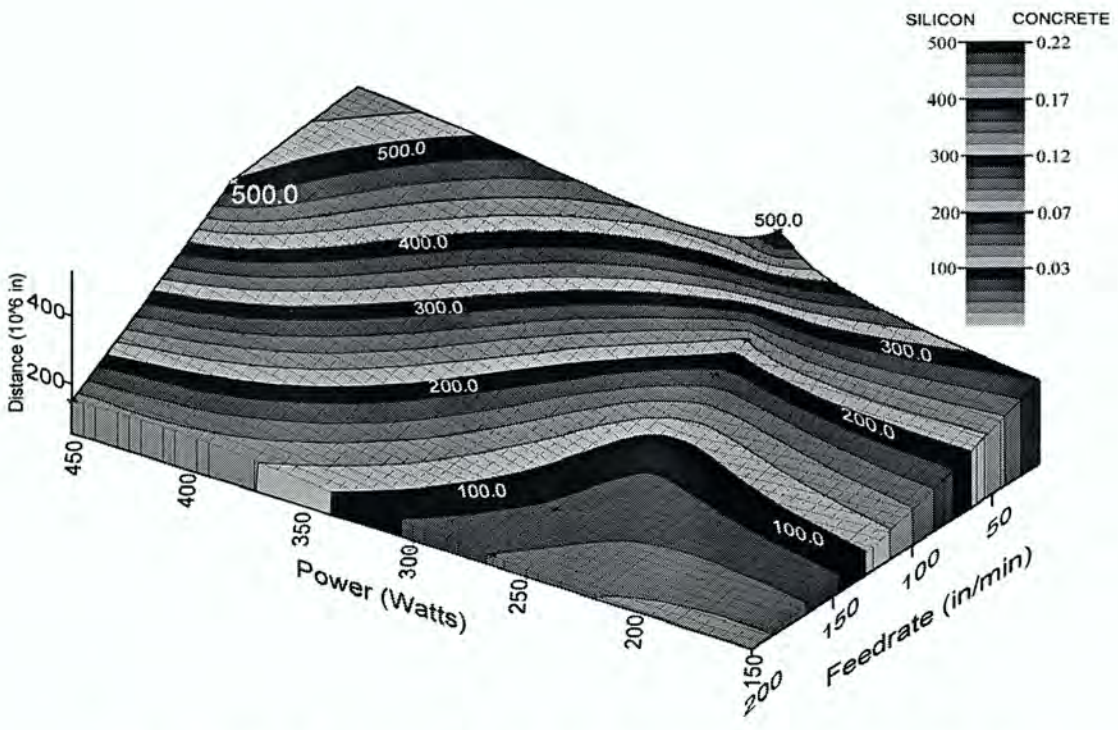


**Figure 7: 3-D plots of cutting silicon with a) Laser alone; (b) LWJ**

### *2.5.3 Concrete*

The 3-D plots of laser parameter effects on depth of cut for concrete are shown in Figure 8. Like other materials, the LWJ did not cut concrete as deep as the laser alone. Also, in both cases no visible cracks were observed during quenching by a water-jet, indicating the concrete's resistance to thermal shock fracture. The results of LWJ cutting of concrete and laser alone are shown in Figure 9. Figure 9a shows that the LWJ sample, initially at room temperature, exhibited almost clean cut with no cracks and negligible slag. While the sample cut with laser alone (Figure 9b) exhibits large amount of slag deposits.

a)

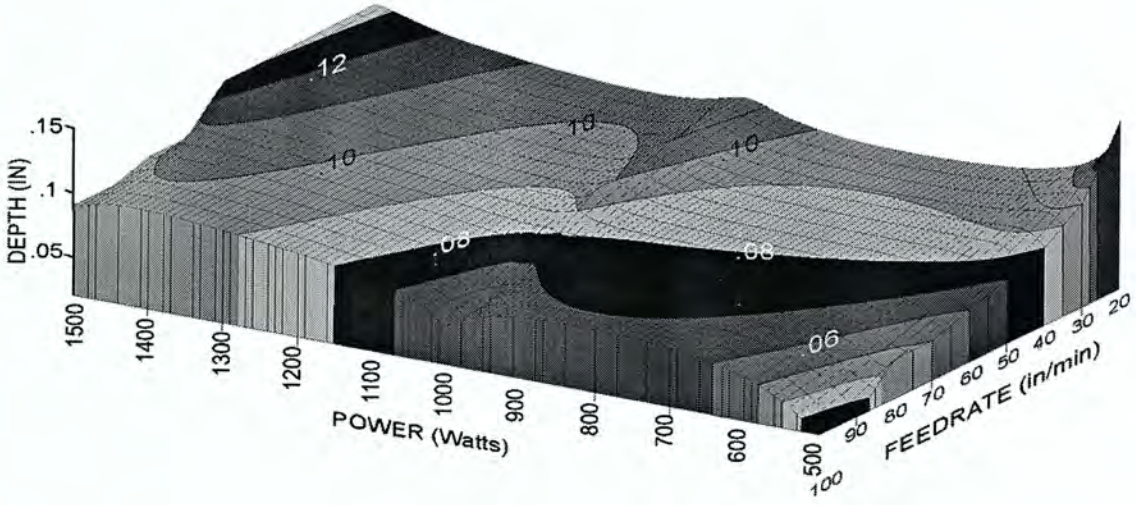


b)

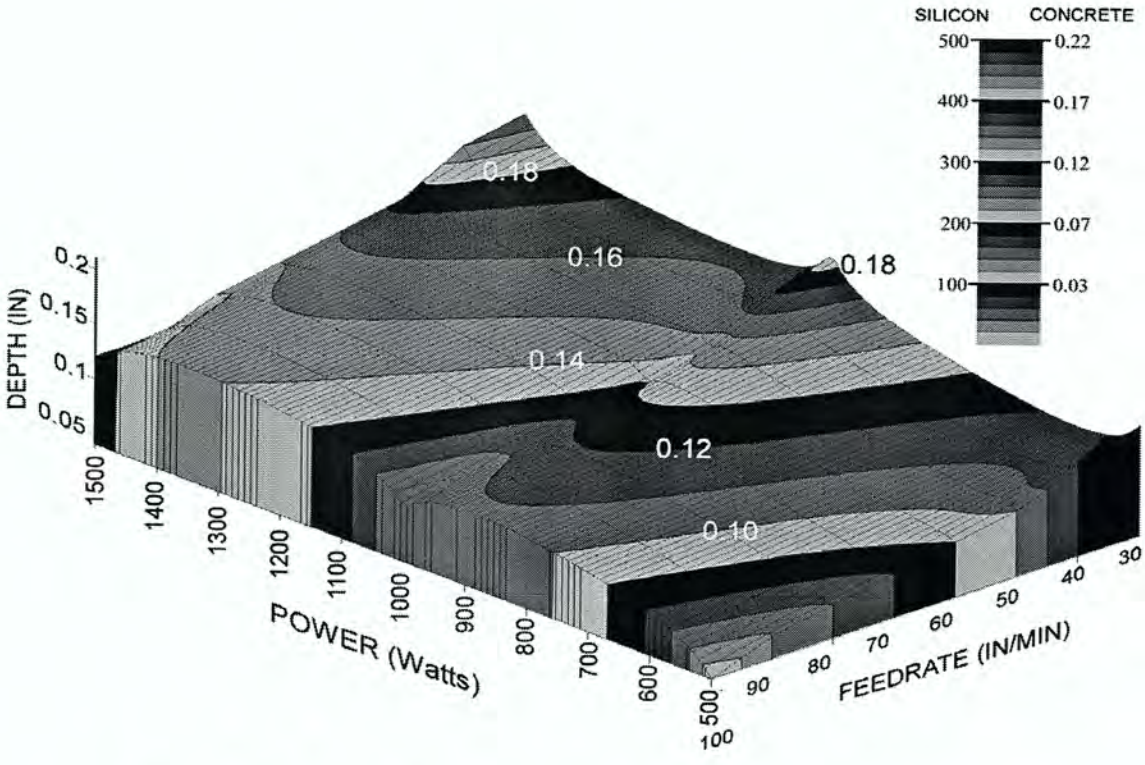


**Figure 8: 3-D plots of cutting concrete with a) LWJ; (b) Laser alone**

Since concrete behaves differently than glass and silicon in terms of thermal cracking and fracturing, other approaches were used to determine the cracking behavior of concrete samples in LWJ. Prior to LWJ cutting, the concrete samples were given two different pretreatments: a) soaked in water and then frozen in a freezer, and b) dipped in liquid nitrogen. It should be noted that only a negligible amount of laser energy is absorbed by water and the samples were frozen uniformly, therefore pre-stresses are assumed negligible and no visible pre-cracks were found. The results of the LWJ cutting frozen concrete sample as well as samples that were cooled in liquid nitrogen are presented in Figure 10. Figure 10a shows that the sample soaked in water and frozen displays even better cut quality than room temperature LWJ cuts but contains channeling cracks. Figure 10b and c show severe cracking observed all along the cut zone of sample cooled with liquid nitrogen. Cracks were distinctively propagated through the limestone component of the concrete. The liquid nitrogen frozen samples have cracked completely through the 6.4 mm thick sample, which would not be the case with just laser alone. The results indicate that concrete does undergo thermal shock fracture but quenching across larger temperature difference is required to induce thermal-shock failure as the operating mechanism.

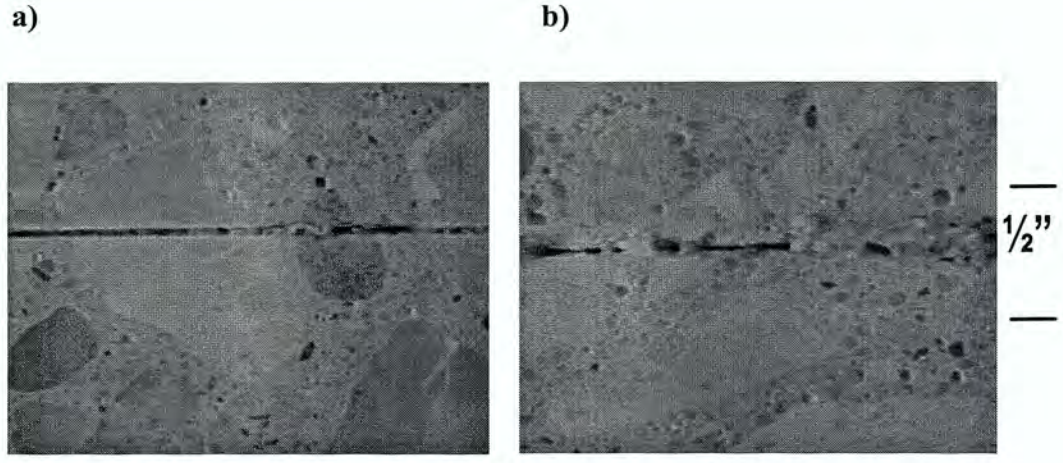


**Figure 9: Surface quality of LWJ and laser cutting of concrete (a) Sample cut with LWJ (b) sample cut by laser alone.**

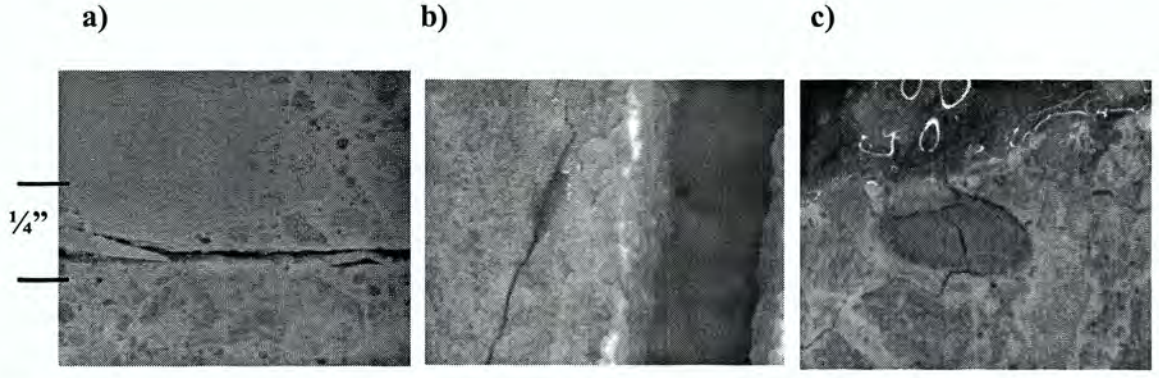


**Figure 10: Cuts and cracks in concrete: a) Sample subjected to large temperature quench by freezing and cutting. b) Cracks that propagate along the cut zone of sample cooled with liquid nitrogen c) cracks that propagated through limestone in the concrete samples cooled with liquid nitrogen.**

## 2.6 Discussion

There is a strong trend toward investigating hybrid manufacturing processes that involve thermal, chemical, electro-chemical and mechanical interactions to meet the challenges of reduction in high machining costs and damages generated during machining [9, 10]. Some of the advantages claimed are complex shapes (airfoil, dies, molds, MEMS), increased

productivity, better surface integrity, tight tolerances, improved surface finish, and less tool wear. The results in the present work assert that the hybrid LWJ has potential to produce clean and more energy efficient cutting through thermal cracking mechanisms. For example, the LWJ produced a spider web pattern of cracks in glass that enabled formation of fine particles of glass; these particles are so weakly bonded such that a stream of water-jet could wash away, leaving a smooth cut. Analysis of LWJ-cut silicon samples further substantiates the positive effect of thermal fracture mechanism on surface roughness. Tsai and Liou also confirm that the surface of traditional laser-cut alumina in thermal stress fracture mode was very smooth compared to the evaporation mode of laser cutting and had very few defects [11].

Laser cutting of brittle materials is accomplished by one of three mechanisms: 1) complete melting and evaporation; 2) partial evaporation to form a deep groove followed by applying a mechanical force or ultrasonic energy to break the material [12]; and 3) controlled fracture (without water-jet) where the laser energy produces a thermal stress causing the material separation similar to a crack extension [13]. The latter technique required much lower laser power than the former methods in cutting alumina and glass using a $CO_2$ laser [11]. Laser methods are usually preferred to mechanical score-and-snap methods that generally leave micro-cracks and residual stresses.

Research results presented here indicate thermal shock phenomenon —where a part subjected to sudden temperature changes is prone to the formation of internal thermal stresses that may weaken the material to the extent of fracture— can be exploited for machining of brittle materials. In the case of ductile metals and polymers, the effect of the internal stresses is overcome by plastic deformation. However in brittle materials, thermal

shock can lend itself to cracking and fracture. Thermal shock is characterized by a number of parameters depending on heat transfer conditions. For low values of Biot modulus as in the present case, the thermal shock resistance, $R$, is given by: $(1-\nu)\sigma k/E\alpha$, where $\nu$ is Poisson's ratio, $\sigma$ is fracture strength, $k$ is thermal conductivity, $E$ is Young's modulus, $\alpha$ is thermal expansion coefficient. Table 1 lists these properties for glass, silicon and concrete [14, 15].

**Table 1. Approximate properties of materials used (ν is taken as 0.2 for all three materials)**

| Material | E GPa | α $10^6$/K | K WmK | σ MPa | R W/m |
|---|---|---|---|---|---|
| Glass | 70 | 0.5 | 20 | 100 | $4.6\times10^4$ |
| Silicon | 160 | 2.3 | 157 | 6000 | $2\times10^6$ |
| Concrete | 35 | 12 | 1.0 | 40 | 76 |

It is interesting to note that despite the low thermal shock resistance, concrete is the most difficult material to crack in LWJ process. This is primarily attributed to the very low thermal diffusivity of concrete that confines the heat diffusion zone to a narrow region.

A one-dimensional heat transport model can be used to predict the surface temperature of materials using Equation 1.

$$T_s = T_0 + \left(I/k\right)\left(\sqrt{4Dt/\pi}\right) \qquad \textbf{(1)}$$

Where $T_0$ is the ambient temperature (300 K), $I$ is the absorbed power density and $t$ is the interaction time. For a customary power density of 500 W/cm$^2$, which is applied with a 200

watt laser, and for an interaction time of 0.2 sec, the surface temperature is estimated to be 2400 K for concrete and 1918 K for silicon. Upon quenching these surfaces, large amount of stresses can be built in the samples. However, thermal diffusivity ($D$) of concrete and silicon are $0.7 \times 10^{-6}$ $m^2$/sec and $100 \times 10^{-6}$ $m^2$/sec respectively. For a laser beam interaction time, $t$, of 0.2 sec, the heat diffusion zone, given by, $\sqrt{4Dt}$, is 0.75 mm and 9 mm for concrete and silicon respectively. Since the tendency to fracture is directly related to the volume of material stressed, the probability for crack formation is much greater in silicon than in concrete.

LWJ produced similar cracking pattern in silicon and glass although silicon exhibited much better quality of cracks. A more controlled pattern of meridian cracks and the absence of spider web cracks were observed in silicon as compared to glass. In addition, silicon produced a nicer quality cut at lower powers. In the case of concrete, a greater thermal gradient was required to produce the desired thermal stress build up. Pre-cooling of concrete was used in this work to obtain the required thermal stresses. Other measures that may be considered for concrete are long interaction time of the laser beam and high intensity beam heating.

We believe that the material removal mechanism in LWJ occurs in a sequence of several steps. First, the laser beam induces a transient temperature field and sets up a compressive stress field. Second, the stress field changes to tension (after the laser beam has passed) due to cooling caused by heat conduction and augmented by water-jet. Third, a crack is initiated and extends from the upper to lower surface resulting in fracture that lags the moving laser beam by a short distance. The fracture is assumed as unstable due to the presence of tensile stress at the crack tip. If the water-jet cooling were absent, then the fracture is said to be

stable due to the compressive stress at the crack tip caused by creep and plastic deformation [11]. Thus, there are distinct differences in the crack propagation mechanisms in thermal fracture mode of laser cutting with and without water-jet.

In evaluating the feasibility of this hybrid LWJ system, the issues that may be considered are: configuration design of two energy sources such as the distance between them, erosive ability of water-jet, and thermal and mechanical properties of brittle materials. In the present work, attention was not paid to the former two aspects that could play a huge role in the energy efficiency and material removal rate. While the present design of LWJ system does not physically cut through most materials as efficiently as the laser alone, more studies on the optimization of this system are needed to fully comprehend its attributes and drawbacks. Preliminary data, however, shows that it could be a viable system to use for cutting certain brittle materials.

## 2.7 Conclusions

A hybrid laser/water-jet (LWJ) cutting using low pressure water was demonstrated as a thermal stress fracture technique for machining glass, silicon and concrete. Spider web cracks in glass, meridian cracks in silicon and channel cracks in concrete were able to cleanly separate the material along the moving path of the laser beam. In the present set-up, the energy efficiency benefits of the hybrid manufacturing were not realized, although the quality of machined cuts were improved as compared to conventional laser cutting. The probable material removal mechanism involves induction of compressive stresses during laser heating followed by a change of stress field from compression to tension during water-jet cooling, leading to the crack initiation and growth from the upper to lower surface. It is

not clear what would be the state of stress at the crack tip and whether material removal occurs through a stable or unstable crack propagation mode. The LWJ has vast potential for machining a variety of brittle materials by offering benefits such as reduced energy, increased cutting speed, improved accuracy and finish, and controlled depth, shape and taper.

## 2.8 Acknowledgments

The authors gratefully acknowledge the financial support for this research provided by the U.S. National Science Foundation under the Grant DMI-0522788.

## 2.9 References

1. H.K. Tönshoff, B. Denkena, H.H. Apmann and J.
Asche, (2003), "Diamond Tools in Stone and Civil Engineering Industry - Cutting Principles, Wear and Applications," *Machining of Natural and Stone Materials, Trans Tech Publications*, p.103.

2. M. Hashish, (1983), "Experimental Studies of Cutting with Abrasive Waterjets," *Proceedings of the 2nd U.S. Water Jet Conference, WJTA*, p. 402

3. H.J. Handewith, R.J. Evans, and E.D. Thimons, (1985), "An Overview of Water-Jet-Assisted Rock Cutting at the Pittsburgh Research Center," Proceedings of the 3rd
U.S. Water Jet Conference, WJTA, Pg 352.

4. R.E.P. Barton and D.H. Saunders, (1982), "Water/Abrasive Jet Cutting of Concrete and Reinforced Concrete," 6th ISJCT, Paper K4.

5. H. Yoshizawa, S. Wignarajah, and H. Saito, (1989), "Laser Beam Cutting of Glass," Transactions of the Japan Welding Society, 20, 1, 36.

6. T. Rümenapp, A. Lenk, (1983), "Laser Beam Cutting of Concrete," Proceedings of the 2nd U.S. Water Jet Conference, WJTA, 257.

7. Synova Water Jet Guided Laser. Laser Micro Jet Information. Home Page. 17. August http://www.synova.ch/

8. D. Perrottet, (2005), "Which Technology: Conventional Dry laser or Water Jet Guided Laser?" LIA Today, March/April, 12, Laser Institute of America, FL.

9. J. Kozak and K. P. Rajurkar, (2000), "Selected Problems of Hybrid Machining Processes. Part 1: Electrochemical Discharge Machining (ECDM/ECAM)", Advances in Manufacturing Science and Technology, (Journal of Polish Academy of Sc., Quarterly), 24, 2, p. 25.

10. K. P. Rajurkar, Zhu, D., and McGeough, J., (1999), "New Developments in Electrochemical Machining," Annals of the CIRP, Vol. 48/2, p.567.

11. C.H. Tsai and C.S. Liou, (2003), "Fracture Mechanism of Laser Cutting With Controlled Fracture." Journal of Manufacturing Science and Engineering, 125, p.519.

12. D.K. Patel and J.D. Baker, (1992), ''Method for Laser Scribing Substrates,'' U.S. patent No. 5,116,641.

13. R.M. Lumley, (1969), "Controlled Separation of Brittle Materials Using a Laser,'' Am. Ceram. Soc. Bull., 48, p.850.

14. M. F. Ashby, (2005), Material Selection in Mechanical Design, Third Edition, Elsevier.

15. T. R. Hsu, (2002), MEMS and Microsystems, McGraw-Hill.

## 2.10 Appendix: Unstable crack propagation in LWJ cutting

A double glass slide set up was used to determine the processing conditions associated with unstable crack growth associated with LWJ cutting. In this experiment, two glass slides were dipped into water and placed one above the other so that there was a thin film of water present between the two slides. This thin layer of water creates a strong thermal gradient on both sides of the glass.

### *2.10.1 Double Glass Slides*

For the laser-alone-cutting method, two slides were stuck together in air and cut with the laser at varying powers and feed rates. The top piece of glass had same cut characteristics as the single glass slides that were cut earlier but the bottom piece of glass had varying characteristics such as melting and heat damage depending on the power and speed. The cut quality was overall good and cracks were not observed in any of these specimens. The double slide set up was then used in LWJ method with both slides immersed in water. The top piece of glass produced similar characteristics to those samples cut by laser alone, but the bottom glass produced significant unstable crack formation. Figure 11 shows the dependence of different crack configuration observed in bottom glass slide as a function of laser power and feed rate.

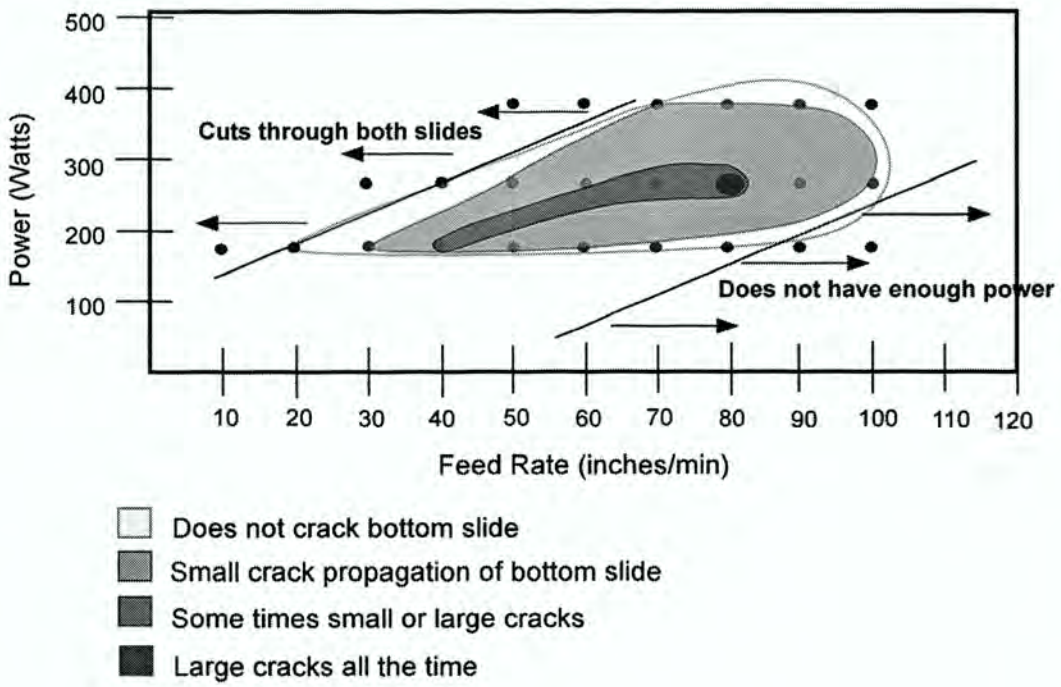


**Figure 11: Map of crack propagation in LWJ cutting of double glass slides depending on power and feed rate.**

The cracks followed the path of the laser beam and propagated from the edge at which the beam started and ended at the opposite side. Figure 12 shows the most common types of cracks, large and small, both of which propagate from the sides of the cut zone. Different sizes of cracks were produced depending on the power and feed rate combination. Generally these cracks are difficult to exactly reproduce except in one set of laser parameters. At 265 watts and 33.9 m/sec (80 inches/min), the bottom piece of glass had cracks (Figure 12a) that was exactly reproduced in several trials. Although there is no sound explanation proposed at this time for this finding, it offers the possibility that the same geometry of crack may be created in LWJ.

a)

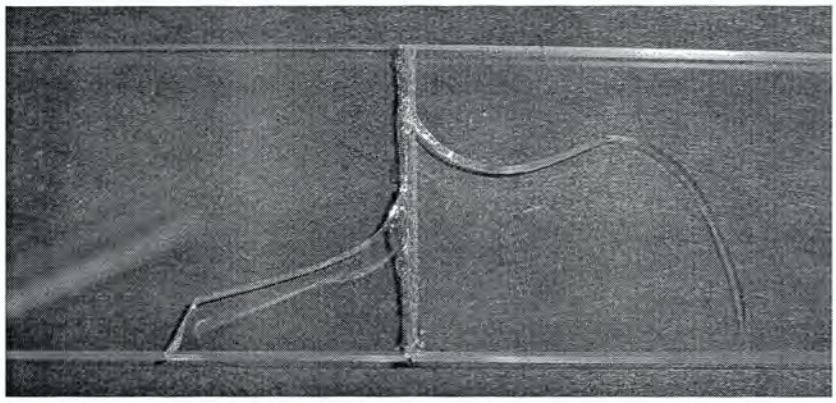

b)

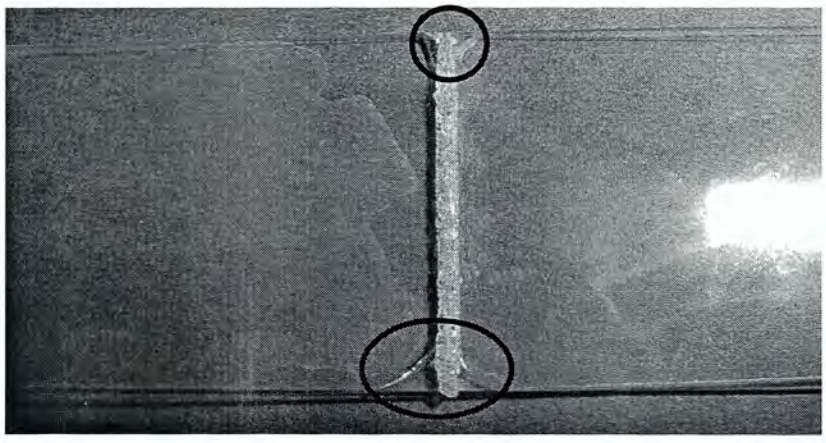

**Figure 12: a) Large crack propagation on double glass slides. b) Small crack propagation on double glass slides.**

Along with the straight lines cut, a circle pattern was also cut on the double glass slide in order to investigate the influence of cut profile on crack mechanisms. In laser-alone-cut samples, the top piece of glass was usually fused to the bottom slide, but no cracks were prevalent in both slides despite the use of various combinations of power and feed rate. In contrast, the circle patterns cut in the LWJ for all powers and feed rates contained cracks

propagating from the same location. Figure 13 shows a photograph of the circle that was cut in LWJ where the locations of crack formation and growth are indicated.

In LWJ cutting of double glass slides, the exact crack location and geometry could be reproduced under a specific combination of laser power and feed rate; this will be useful in fracture mechanics analysis of the material removal mechanism.

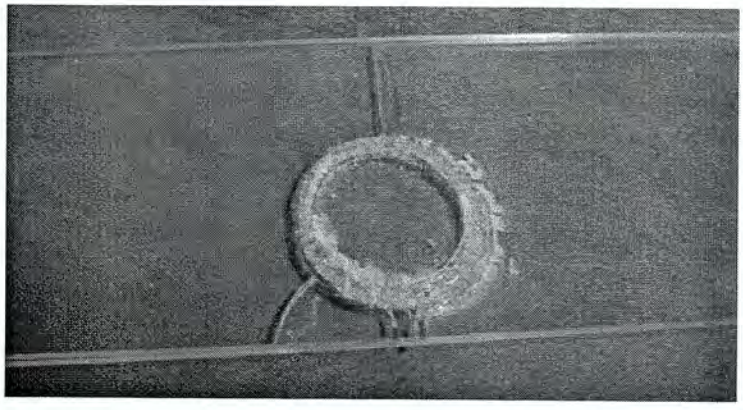

**Figure 13: Circle cut on the double glass with reproducible cracks in LWJ.**

# Chapter 3: Water–Assisted Laser Thermal Shock Machining of Alumina

A paper to be submitted to International Journal of Machine Tools and Manufacturing

Christopher Barnes, Pranav Shrotriya and Pal Molian
Laboratory for Lasers, MEMS and Nanotechnology
Department of Mechanical Engineering
Iowa State University
Ames, IA 50011

**Keywords**

Laser; Cutting; Processing; Alumina; Thermal shock fracture; Water

## 3.1 Abstract

A combined experimental and computational approach was undertaken to investigate water-assisted laser cutting of 96% pure alumina specimens through controlled thermal shock fracture mechanism. A low-power $CO_2$ laser (<300 W) was used for localized heating and scribing of alumina samples followed by water quenching to induce thermal stress cracking. In order to elucidate the cutting mechanisms and identify the regime of processing conditions suitable for controlled fracture, laser cutting experiments were performed under two different environments: water-assisted laser cutting and dry laser cutting. Temperature profiles of the heat affected zones were obtained using thermocouples and data acquisition system. Finite element analysis was applied to predict the temperature and thermal stress distributions developed during both water-assisted and dry laser cutting operations. Temperature histories of the samples recorded during cutting were compared with numerical model predictions to

determine heat transfer parameters associated with wet and dry laser cutting of alumina samples. Both experimental data and numerical analysis indicate that water quenching makes a substantial difference in thermal stress distribution which governs the ability to control the fracturing of alumina. This can in turn, produce higher feed rates than previously reported in laser machining of alumina.

### 3.2 Introduction

Alumina (aluminum oxide), the most common structural ceramic, is widely used for a variety of applications ranging from microelectronics to prosthetics because of desirable properties such as: high hardness, low chemical reactivity, high volume receptivity at elevated temperatures, low density, low thermal conductivity, and ultrafine finishing capability. Most of these applications require faster processing, tighter dimensional tolerance and excellent surface integrity, therefore controlled processing and manufacturing of alumina becomes very important. Traditional cutting methods for alumina are limited by its brittleness, hardness and low thermal expansion, leading to: increased vulnerability to workpiece fracture; great loss of workpiece material; tool failure; difficulty in achieving the design requirements of high precision and excellent surface integrity; need for high power sources; and need for regular maintenance due to wear [1-4]. It is crucial to develop non-traditional machining processes that can fabricate alumina parts at a relativity high rate, while eliminating the fractures and breakages associated with traditional manufacturing methods [5, 6]. Consequently, $CO_2$ laser cutting has become an effective industrial technique for producing useful shapes in alumina due to its localized heating effect and non-contact nature over mechanical methods [7].

The $CO_2$ laser is the most precise and versatile tool for fabricating brittle ceramic substrates like alumina. However, the $CO_2$ laser has still not reached its full potential. A laser offers many distinct advantages in cutting materials such as features of any planar shape, tight tolerances (± 0.01 mm), soft tooling, flexibility in design layout, quick turnaround and low cost. However, the use of lasers does not necessarily preclude damage and/or fracture of the workpiece due to uncontrolled cracking.

$CO_2$ laser cutting of alumina can be accomplished by three different methods: 1) melting and evaporation where the melt layer is blown off by a high-pressure (80 to 90 psi) gas stream; 2) partial evaporation to form a deep groove followed by applying a mechanical force or ultrasonic energy to break the material [8]; and 3) controlled thermal stress fracture where the laser energy produces a thermal stress causing the material separation similar to a crack extension [9, 10]. The evaporation/melting mode of material removal requires extreme power lasers (> 1000 W), leading to collateral thermal damages such as residual stresses, heat affected zone, recast layer, uncontrolled fracture etc. In contrast, controlled thermal stress fracture mode of material removal can be achieved at low powers (15-20 W) but suffers from slowness and narrow range of process parameters [9, 11-14]. In addition, the scattering errors associated with the process often promote uncontrolled crack propagation. Laser methods are preferred to mechanical score-and-snap methods that generally leave micro-cracks and residual stresses.

Controlled thermal fracture mechanism is an energy efficient process as low-powered lasers operating below the melt/ablation threshold are utilized for localized heating of workpiece and a gas stream is added for cooling the heated zone, leading to fracture of sample. Unfortunately, control of the fracture path necessitates use of slow feed rates (~ 5-30

mm/sec, see ref [9]). In order to improve the productivity, Segall and co-workers have reported a dual-beam laser cutting process where one beam causes pre-scoring of the workpiece surface while the other beam fractures the sample [11]. Pre-score groove on the sample surface serves to guide thermal stress-induced crack. As compared to single beam controlled fracture machining, dual beam machining produced a modest increase in the feed rate of alumina (~150%) [11].

In order to satisfy the pressing need of improving alumina cutting speed while maintaining excellent surface integrity and tighter tolerances, a novel approach of combining laser and water quenching is undertaken in this work. The laser heating creates temperature gradient in a zone approximately equal to thermal diffusion depth and rapid quenching of that zone by the water develops thermal stresses that fracture this zone. Thermal stresses arise due to non-uniform expansion of the material associated with localized heating and cooling [16]. Rapid cooling rather than rapid heating inflicts most of thermal shock damage since the induced surface stresses are tensile in nature during rapid cooling. Rapid quenching of the sample also limits the diffusion of heat away from the laser heated zone. Confinement of heat in small zone ensures that only a small volume of the workpiece material is subjected to non-uniform expansion (during heating) and contraction (during cooling) leading to greater control over sample fracture. As a result, water-assisted laser machining is expected to allow higher feed rates during cutting of alumina. In addition, it avoids the formation of liquid and gaseous phases, making the cutting process more energy efficient and free from hazardous emission [13]. Thus, controlled thermal fracturing obtainable through water-assisted laser cutting can meet the challenges of higher feed rate, reduced energy and improved environment in the shaping of alumina.

### 3.3 Experimental Procedure

A 1.5 kW (maximum power) continuous wave $CO_2$ laser with an *x-y* computer numerical controlled (CNC) positioning table was used for cutting experiments. Samples used for cutting experiments were 96% alumina with nominal dimensions of 0.5 mm thick, 25 mm wide and 100 mm long. 96% alumina is an excellent substrate material for cost-effective laser processing and represents over 90% of the microelectronic circuits and multichip modules [17]. Table 1 lists the mechanical, physical, thermal and electrical properties of 96% alumina.

During the cutting tests, the laser beam was focused on the specimen surface to a spot size of ~0.25 mm using a 127 mm (5 in.) focal length lens. All the samples were secured using a custom-made fixture. For water-assisted laser machining, sample fixture was set into a tub of water held at 18°C such that the alumina samples were approximately 1-2 mm below water surface. A constant stream of air flow (<2 psi) was maintained through the laser nozzle in order to prevent spatter reaching the optical elements. The air stream created a dry spot on the sample approximately 5 mm in diameter and enabled the laser to hit the alumina sample without being deflected by or diffused in the water. However, as the laser beam is swept away from the spot, water moves in causing thermal quenching. A schematic of this configuration is presented in Figure 1.

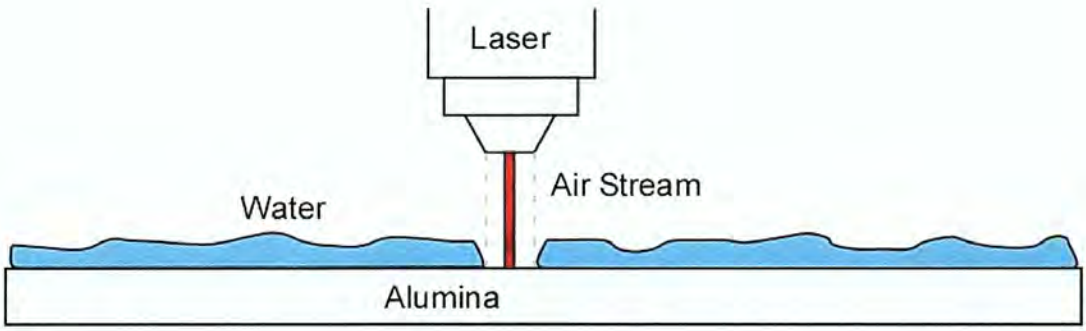


**Figure 1: Schematic of laser and air stream with water layer (not to scale).**

During cutting experiments, the laser beam was made to begin irradiation outside of the alumina sample and then translated into the sample for a distance of approximately 20 mm along the 25 mm width of the sample. Water-assisted machining experiments were carried out for several combinations of laser power and feed rates as shown in Table 2. Alumina samples were also machined using dry laser cutting under the same experimental conditions. After each cutting test, the sample surface was closely examined and then grouped into four different categories based on the sample fracture characteristic: cut-through, scribed, controlled cracking and uncontrolled cracking. Representative images of samples demonstrating controlled and uncontrolled cracking are shown in Figure 2. Experimental observations were utilized to create process maps for identification of the range of processing conditions required for controlled thermal fracture of alumina samples.

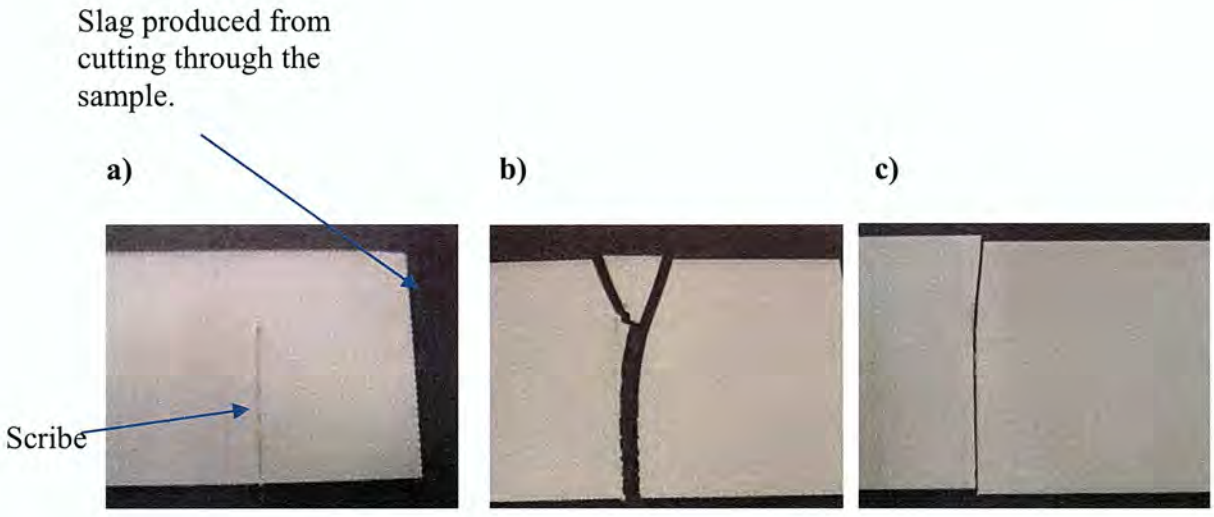


**Figure 2: Photographs of slag and cracks observed in the laser-cut alumina samples: a) Slag produced from cutting through the alumina sample in melt/evaporation mode. b) Uncontrolled cracking in thermal shock mode. c) Controlled cracking of alumina sample in thermal shock mode.**

In order to clarify mechanisms governing thermal stress development during both water-assisted and dry laser cutting, real time temperature readings of alumina samples were taken. Thermocouples (1/16" diameter, K type) were mounted on the surface of the alumina at the locations 1 mm, 2 mm, and 3 mm away from the laser-cutting zone and temperature history at each point was recorded using a data acquisition system. The thermocouples were attached to the samples with a high thermal conductive adhesive tape. In order to ensure that the sample heating is symmetrical about the cutting line, experiments were performed with thermocouples mounted on both sides of the laser-cut zone. Temperature data was found to be symmetrical about the cutting line. Temperature readings were taken from the start of the experiment until the sample had cooled to the ambient temperature. Temperature measurements were repeated a number of times to ensure consistency and repeatability.

Figure 3a shows a schematic of the data acquisition system set up while Figure 3b shows a photograph of laser cutting nozzle, water tub and sample fixture.

**a)**

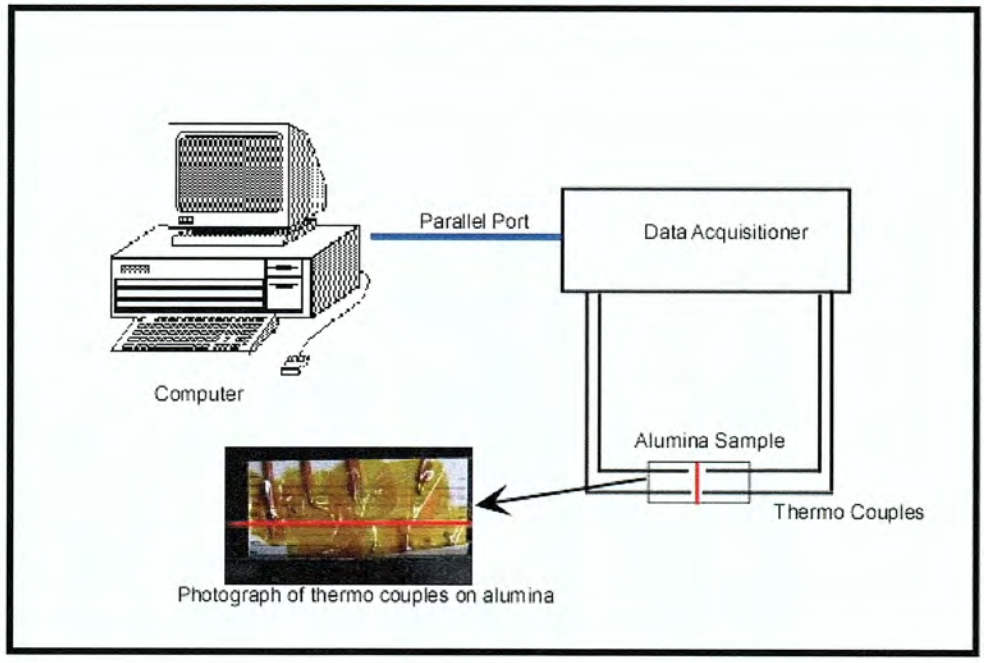

**b)**

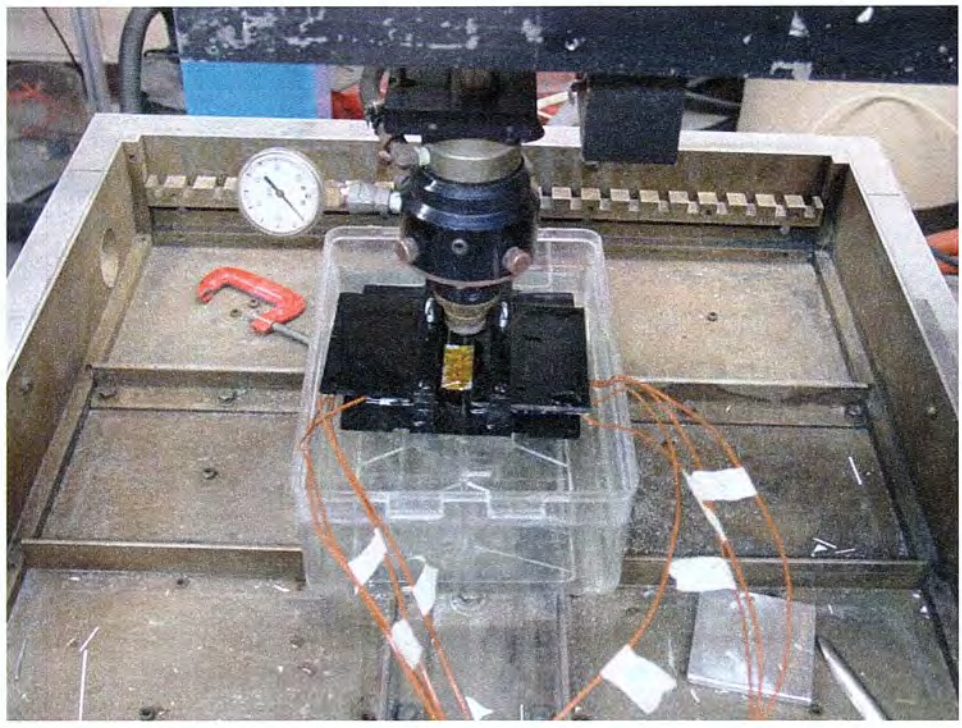

**Figure 3: a) Schematic of data-acquisition system and alumina sample embedded with thermocouples; b) Photograph of laser cutting nozzle, water tub and sample fixture along with thermocouple leads.**

### 3.4 Numerical Analysis

Finite element analysis was applied to predict the temperatures and stress distributions in the sample, more specifically in the heat affected zone [18]. An axis-symmetric model was formulated to determine the effects of localized heating and cooling of the samples in both water-assisted and dry machining environments. Numerical simulation was performed in two steps: first is the localized heating due to incident laser beam and second is cooling of the heated zone to ambient temperature in air or water depending on machining set up. Transient thermal analysis was used to calculate temperature fields and associated stress fields for both steps. A schematic of the thermo-elastic model is presented in Figure 4.

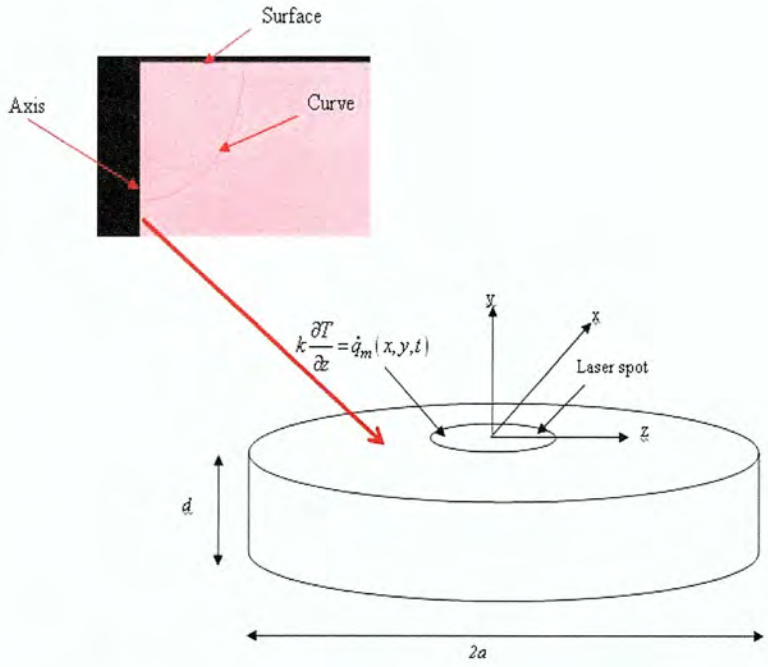


**Figure 4: Schematic of axis-symmetric thermo-elastic problem**

The governing equations and boundary conditions for obtaining temperature distribution in the axis-symmetric analysis are given by:

$$\rho C_p \frac{\partial T}{\partial t} = \frac{1}{r}\frac{\partial}{\partial r}\left(kr\frac{\partial T}{\partial r}\right)+\frac{\partial}{\partial z}\left(k\frac{\partial T}{\partial z}\right)$$

$$-k\frac{\partial T}{\partial r}=0 \text{ at } r=0$$

$$-k\frac{\partial T}{\partial r}=0 \text{ at } r=a$$

$$-k\frac{\partial T}{\partial z}=0 \text{ at } z=0 \text{ Bottom surface} \quad ; \qquad (1)$$

$$-k\frac{\partial T}{\partial z}=\dot{q}_m \text{ at } z=d \text{ Top surface}$$

$$T(r,z,0)=T_0$$

where $\rho$ is the temperature dependent density, $k$ is the thermal conductivity and $C_p$ is the specific heat. In order to simulate the dry and water-assisted laser cutting processes, a circular spot of radius, $b$, on the top surface will be irradiated by a laser beam for a short period of time, $t_1$, and subsequently, the workpiece will be cooled in air or water. In the numerical model, flux on the top surface, $\dot{q}_m$, will be utilized to simulate the laser heating and subsequent cooling:

$$\begin{aligned} \dot{q}_m\left(r, 0 < t \le t_1\right) &= \begin{cases} a_s P / \pi b^2 & \text{if } x^2 + y^2 \le b^2 \\ h\{T(r,d,t) - T_0\} & \text{if } x^2 + y^2 \le b^2 ; \end{cases} \\ \dot{q}_m\left(r, t > t_1\right) &= h\{T(r,d,t) - T_0\} \end{aligned} \tag{2}$$

where $a_s$ is workpiece absorption coefficient; $P$ is power of the laser irradiating the surface; $b$ is the radius of the laser spot and $h$ is the temperature dependent heat transfer coefficient of the surface. In the first step, it is assumed that $a_s = 0.72$ i.e. 72% of the laser incident energy is absorbed in the sample. The assumption is based on approximating: losses due to transmission through optical system; and losses due to laser deflection and scattering; temperature dependent reflectivity at the sample surface and losses due to ablation/melting of sample surface. Reflectivity of a laser beam from the sample surface held at temperature, $T$ is given by:

$$\boldsymbol{R} = 1 - \left( 4 \left( \frac{\pi \boldsymbol{C} \rho \varepsilon_0}{\lambda} \right)^{1/2} \right) \left( \frac{\boldsymbol{T}_0}{\boldsymbol{T}} \right)^{0.1673} \tag{3}$$

where $T_0$ is the room temperature, $R$ is reflectivity, $C$ is the velocity of light, $\rho$ is electrical resistivity, $\varepsilon_0$ is vacuum permittivity and $\lambda$ is wavelength of laser beam. Equation (3) is valid only in the solid state heating. From the solution to Equation (1), we can obtain the

temperature distribution $T(r, z)$ as a function of time. Due to the concentrated nature of heat source, temperature gradients are developed through out the material leading to thermal stresses and strains. The strains are computed using the following equations:

$$\varepsilon_{xx} = \frac{1}{E}\left(\sigma_{xx} - \nu(\sigma_{yy} + \sigma_{zz})\right) + \alpha(T(x,y,z,t) - T_i)$$
$$\varepsilon_{xx} = \frac{1}{E}\left(\sigma_{yy} - \nu(\sigma_{xx} + \sigma_{zz})\right) + \alpha(T(x,y,z,t) - T_i) \qquad (4)$$
$$\varepsilon_{zz} = \frac{1}{E}\left(\sigma_{zz} - \nu(\sigma yy + \sigma xx)\right) + \alpha(T(x,y,z,t) - T_i)$$

where α is the thermal expansion coefficient. Thus, the transient strain distribution can be calculated by solving the equilibrium equations. The stresses are then calculated by solving the equilibrium equations with boundary conditions and no external forces. The finite element model is also applied to determine the transient temperature and stress distributions corresponding to various processing parameters like laser power, cutting speed, and cooling conditions.

Finite element model is composed of 6-noded quadratic modified axi-symmetric triangular elements. The model was partitioned around the heat affected zone and mesh was refined in that area as well. The refined mesh and partitioned zone can be seen in Figures 4 and 5, respectively.

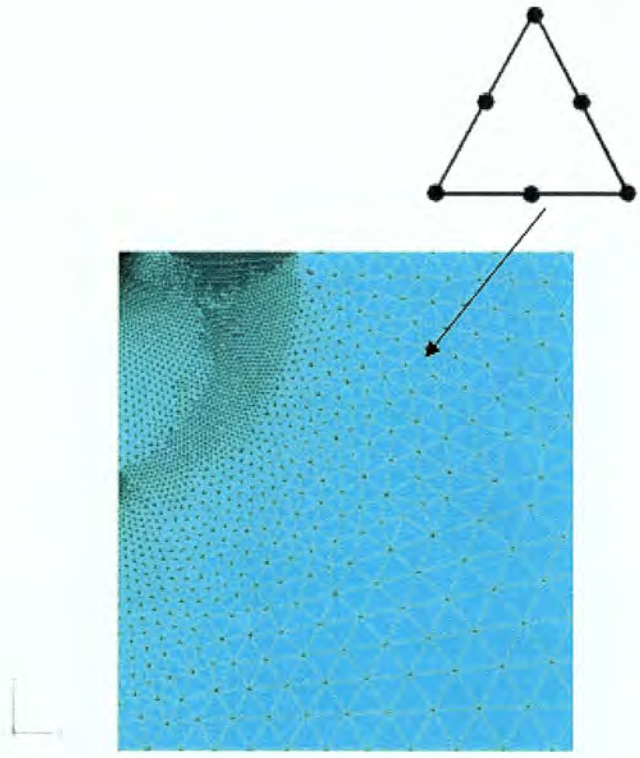

**Figure 5. The mesh around and at the heat affect zone and a 6-node triangular element.**

Numerical simulations were performed under two different types of conditions. The first was to simulate the quenching of alumina with water after being heated with the $CO_2$ laser and the second was the simulation of the alumina cooling with air after being heated with the laser. During these simulations the laser interaction time and properties of the alumina were kept the same. The heat transfer coefficient of the thin film was changed to correspond to the particular properties of the air or water that cooled the sample. Simulations were performed for the following processing conditions: input laser power of 100, 200, and 300 watts with a feed rate of 220 inches/minute for both water-assisted laser cutting as well as dry laser cutting. This particular feed rate was chosen because as the laser power at this feed rate was

increased, the sample fracture characteristics distinctly changed from scribing to controlled cracking and finally to uncontrolled cracking.

### 3.5 Results and Discussion

Sample fracture characteristic plots of feed rate versus power were created for alumina corresponding to both water-assisted and dry laser machining operations and are presented in Figures 6a and 6b, respectively. The material removal characteristics were separated into four categories: partial cutting with no cracks (scribing (shown in Figure 2(a))), controlled cracking (shown in Figure 2(b)), uncontrolled cracking (shown in Figure 2(c)), and complete cutting with no cracks (cut-through). The cut-through and scribing modes are essentially due to melting and evaporation mechanisms of material removal while the controlled cracking and uncontrolled cracking modes are associated with thermal stress induced fracture.

At highest power and slowest feed rate (300 watts and 42 mm/sec), the dry laser cut samples exhibited "cut through" while no other processing conditions in the range tested showed this result (Figure 6a). The samples cut using water-assisted laser cutting do not exhibit "cut through", suggesting that the experimental conditions were below the evaporation/melt threshold (Figure 6b).

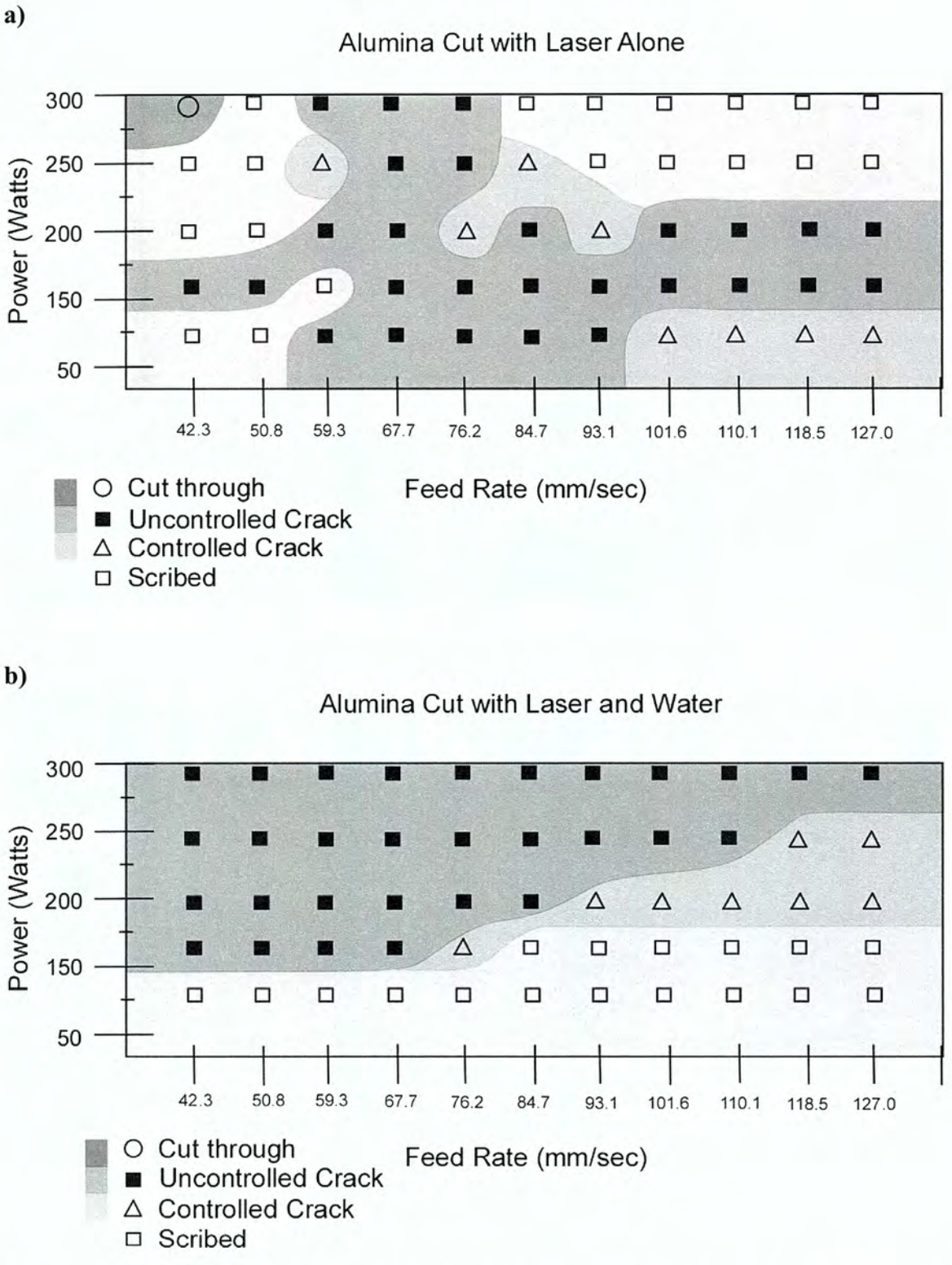


**Figure 6: Process maps based on power and feed rate. a) Alumina cut with laser alone b) Alumina cut with laser and water.**

The data collected for the dry laser cutting of alumina had inconsistent results, although many of the experiments at random grid points were retested for consistency. The data does not seem to have any clear divisions between uncontrolled cracking and controlled cracking (Figure 6a). While the data for the alumina that was cut with the water-assisted laser displayed consistent results depending on the power of the laser and the sample feed rate. At lower powers and faster feed rates, the samples were scribed with no evidence of cracks. Above this point all the samples had cracked, however, only at the faster feed rates, the samples exhibited controlled cracking. The overall cut quality of all alumina samples for both dry and wet laser cutting was good. Samples that "cut through" exhibited slag on the bottom and samples that "scribed" exhibited slag on the top of the sample. Samples that fractured produced a good quality, clean cut with no slag.

Experimental results indicate that during water-assisted laser machining controlled cracking of alumina can be obtained for feed rate range from 75 mm/sec to 125 mm/sec. Tsai and Lou [9] studied the controlled fracture of alumina with low power lasers (~15W) and gas jet assisted cooling of the irradiated zone. Controlled fracturing of alumina could only be obtained for very slow feed rates (~ 5-30 mm/sec, see ref [9]). Segall and co-workers [11] utilized a dual-beam laser cutting process for controlled fracturing of alumina and established a modest increase in the feed rate (~180%) as compared to single beam cutting. Experiments reported in this study demonstrate controlled fracture of alumina during water-assisted machining at feed rates that are almost five times greater than single beam cutting. Hence, water-assisted laser machining can be exploited for cutting of alumina at rapid feed rates.

The laser power, spot size and feed rate were utilized to estimate energy density threshold required for different fracture characteristics associated with water-assisted laser cutting (shown in Figure 6b). Energy density for a particular laser power ($P$), laser spot size ($r$) and feedrate ($v$) was determined according to the following equation:

$$Energydensity = \frac{(2r)(P)}{v\pi r^2} \tag{5}$$

Experimental results indicate that an energy input of approximately 637.6 J/cm$^2$ is required to initiate controlled cracking of samples (Figure 2c). Above 637.6 J/cm$^2$ the samples underwent uncontrollable cracking and below this threshold the samples could only be scribed. Transition of sample fracture characteristics from scribing to controlled cracking at the energy density threshold and from controlled cracking to uncontrolled cracking above that threshold is consistently observed for all the experimental conditions.

Finite element analysis was used to identify the stress distributions associated with water-assisted laser cutting and dry laser cutting for processing conditions that correspond to below, equal and above the identified energy density threshold. Experimentally measured sample temperature histories were used to approximate the heat transfer coefficients associated with air and water cooling. For each processing condition, numerical analysis was utilized to predict the transient temperature distributions on the sample surface. Numerical predictions were compared to experimental measurements to identify the heat transfer coefficients that closely approximated the measured temperature history. Surface heat transfer coefficients of 1000 W/m$^2$K and 6310 W/m$^2$K closely approximated the measured temperature histories for air cooling and water cooling conditions, respectively. Experimental measurements of sample surface temperature are compared with numerical predictions for dry and water-

assisted laser cutting shown in Figures 7a and 7b, respectively. Temperature measurements were taken in a number of locations on the sample surface. For the water cooling, all the numerical predictions based on approximated heat transfer coefficients closely follow the measured temperature histories. For the air cooling, numerical predictions are close to experimental measurements performed away from the laser cutting path but there is a significant disparity for measurements performed close to laser cutting path. Numerical predictions are close to experimental measurements for all the cases associated with modest temperature excursions.

The discrepancy between numerical predictions and measurements may be due to inadequate thermocouples and inaccurate modeling assumptions. Thermocouples (1/16" bulb diameter) have significant thermal inertia and may not be able to record the rapid rise in temperature close to laser cutting zone during dry laser cutting. In addition, numerical predictions of temperature history in this simple model are based on an assumption of temperature independent heat transfer coefficient. It is expected that increase in surface temperature will lead to increased convective heat transfer and a temperature dependent heat transfer coefficient may be necessary to accurately model the air cooling. Temperature dependent heat transfer coefficient is beyond the scope of the simple model presented in this study. Thermocouples with lower thermal inertia and temperature dependent heat transfer coefficients will be utilized in future investigations in order to overcome the discussed limitations.

As shown in Figures 7a and 7b, alumina samples machined using dry laser cutting cooled at a much slower rate then the samples machined using water-assisted laser cutting, due to the slower heat dissipation from the surface to air. During water-assisted laser machining,

laser heated zone is rapidly quenched thus only a small volume of the material is heated due to diffusion. In contrast during dry laser cutting, slow cooling of the sample surface leads to heating up of a larger volume of material due to diffusion away from the laser heated zone. Consequently, sample stress distributions are different during water-assisted laser and dry laser machining. Representative contour plots of the predicted radial stress distribution during air and water cooling are presented in Figures 8a and 8b, respectively.

**a)**

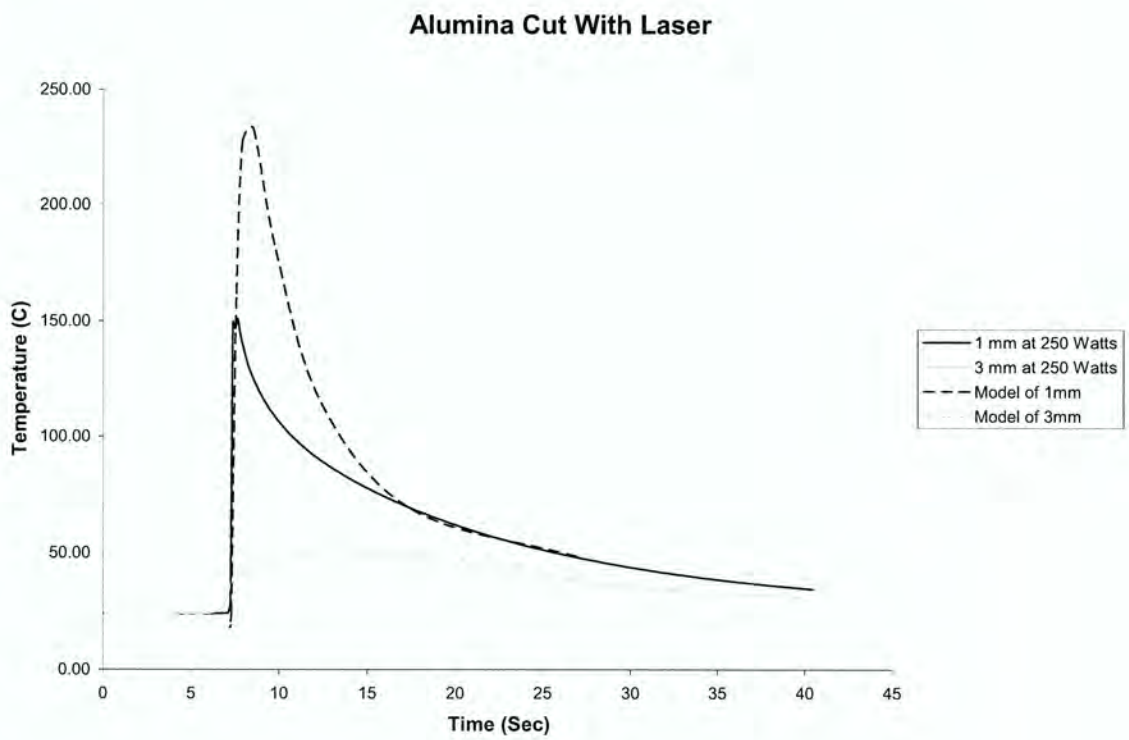

**b)**

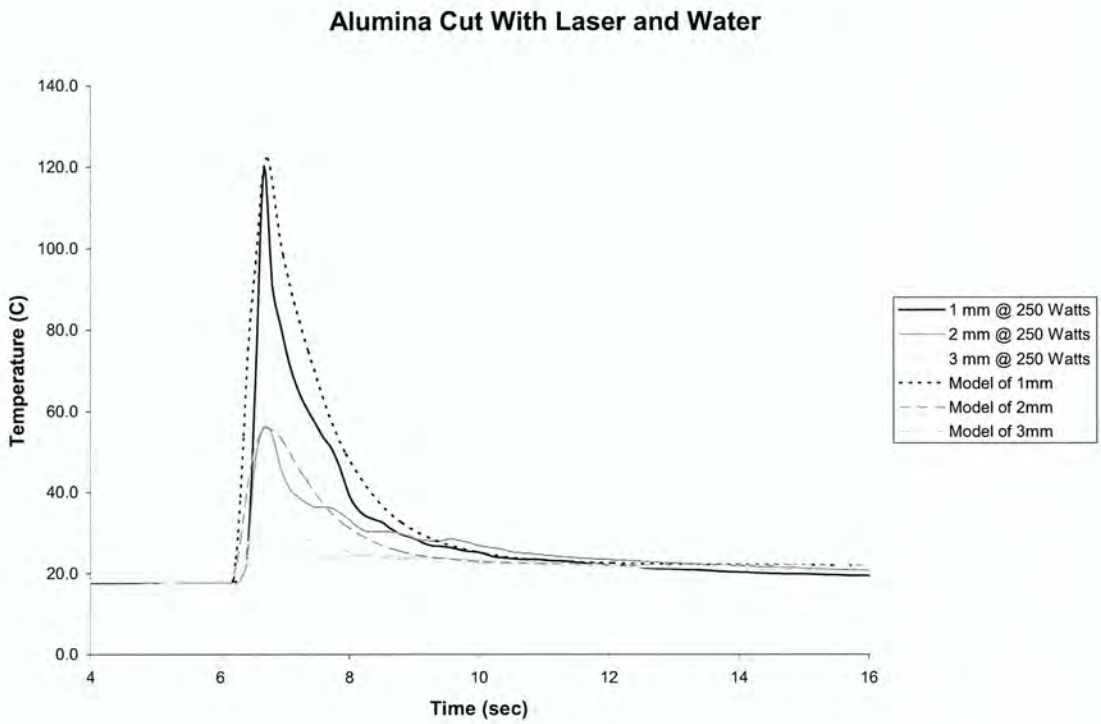


**Figure 7: Experimental and numerical graphs of temperature vs. time. a) Alumina cut with laser alone b) Alumina cut with laser and water.**

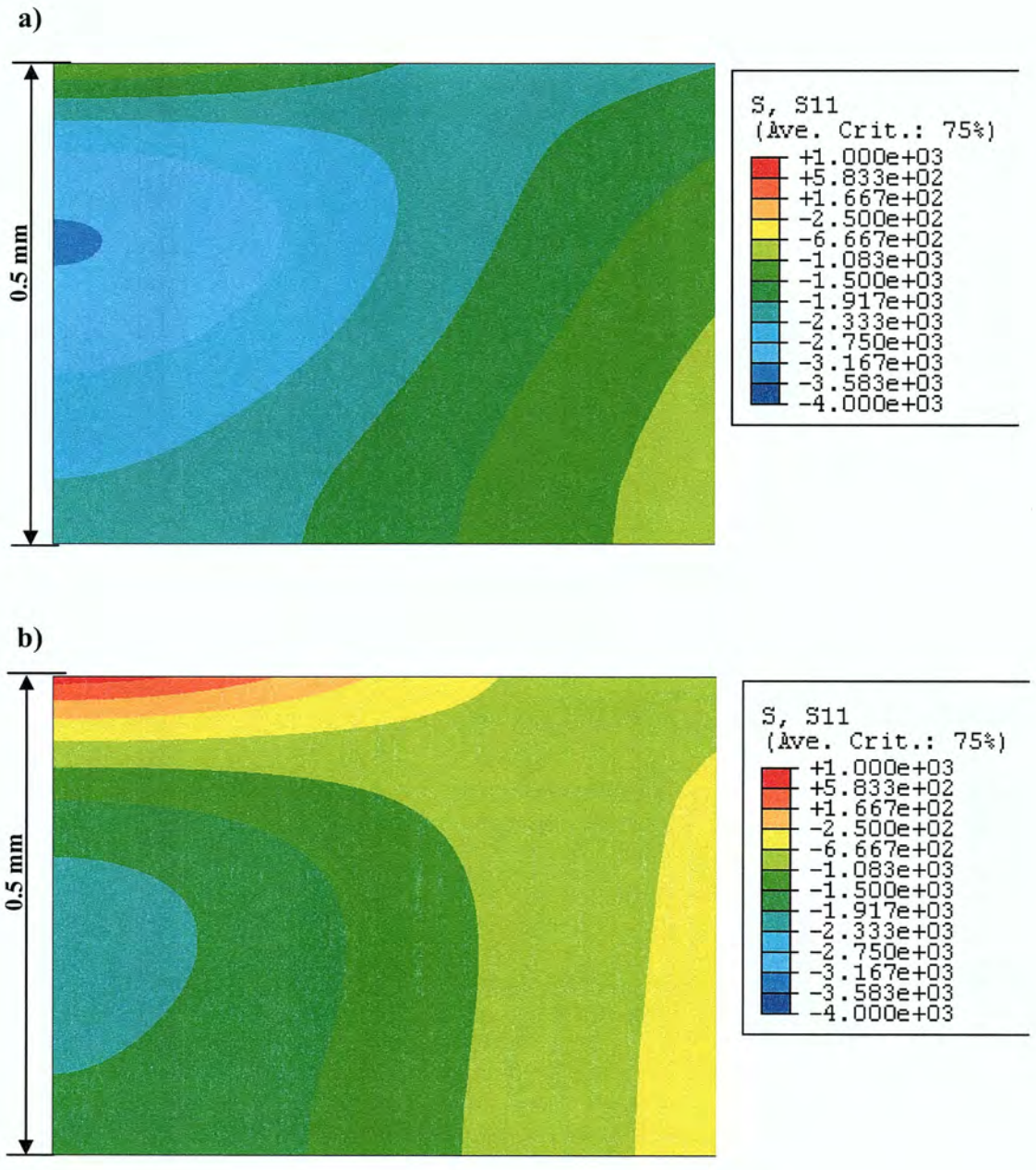


**Figure 8: Contours of radial stresses in the alumina samples with 637.6 J/cm$^2$ of energy input at .330 seconds after cooling (stresses in MPa). a) Stresses using air to cool sample. b) Stresses using water to cool sample.**

Time histories of the radial stress at three different locations (surface, middle and bottom) along the sample axis are plotted in Figures 9a and 9b for air and water cooling respectively. During laser irradiation of surface, a zone approximately equal to thermal diffusion depth is rapidly heated from the ambient temperature of $T_0$ = 18°C to $T_f \approx$ 2000°C. Due to the restraint of the surrounding material, large compressive stresses develop in the heated zone while the rest of the sample is subjected to tensile stresses. As the sample is cooled in air, the large compressive stress in the heat affected zone decrease with time. Due to the slow cooling rate, temperature gradients in the sample do not change sign and consequently, radial stresses in the heat affected zone are always compressive. Pre-existing flaws on the material surface are not expected to grow into crack and lead to fracture of the sample surface because of the radial compressive stress distribution in the heat affected zone. Experimentally observations of sample fracture may be due to material ablation and surface damage induced during the laser irradiation.

When the laser irradiated zone is quenched in water, sample surface is rapidly cooled resulting in thermal shock i.e. development of tensile radial stresses in the heat affected zone. The large tensile stresses associated with rapid cooling of material are responsible for propagation of existing flaws into cracks and fracture of the work-piece. Magnitudes of tensile stresses induced during thermal shock depend on the input energy density during laser irradiation. The maximum tensile stress in the heat affected zone in the samples that were cut in water-assisted cutting were 265 MPa, 767 MPa and 1250 MPa respectively after a 20 second cooling period for input energy density of 328.2 J/cm$^2$, 637.6 J/cm$^2$ and 984.2 J/cm$^2$, respectively. As shown in contour plot of radial stress, a small volume of the sample surface

is subjected to tensile stresses during the water cooling. The ultimate tensile strength of alumina is approximately 220 MPa. At the lowest power density a very small volume of the material is loaded above the ultimate strength of material. As the power density is increased larger and larger volume of material are stressed above the ultimate tensile strength. Since the tendency to fracture is directly related to the volume of material stressed, the probability for crack formation increases as the input energy density is increased resulting in transition form scribing to controlled cracking and ultimately to uncontrolled cracking.

**a)**

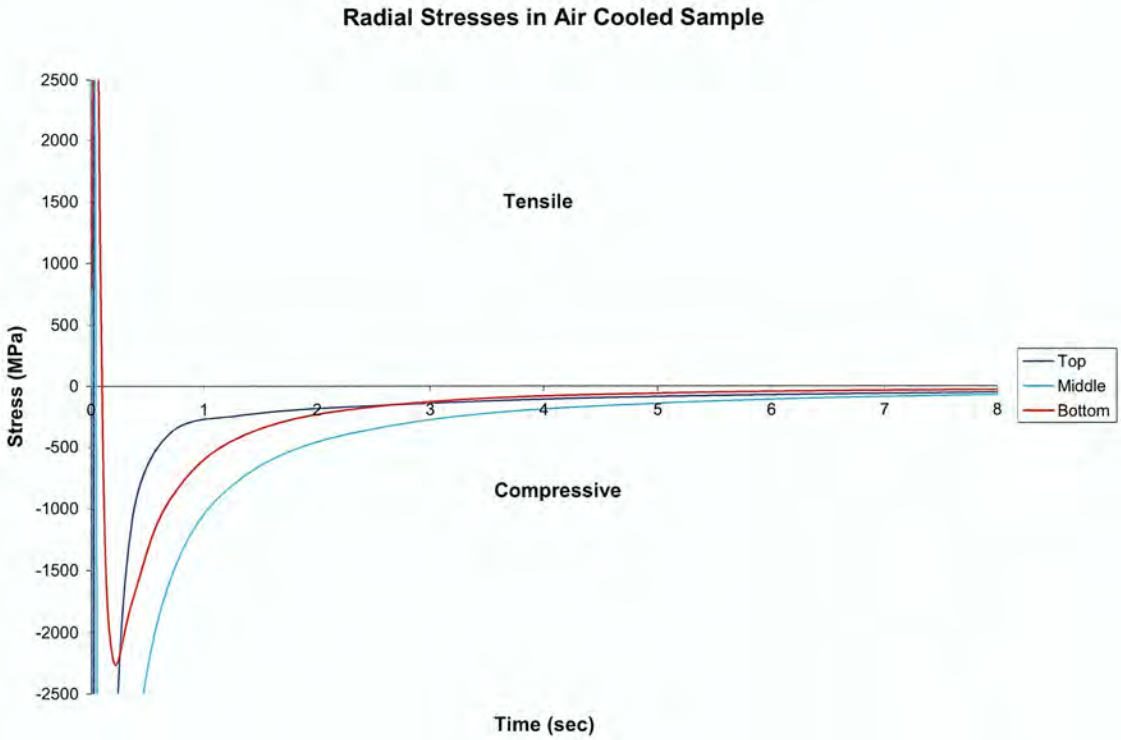

**b)**

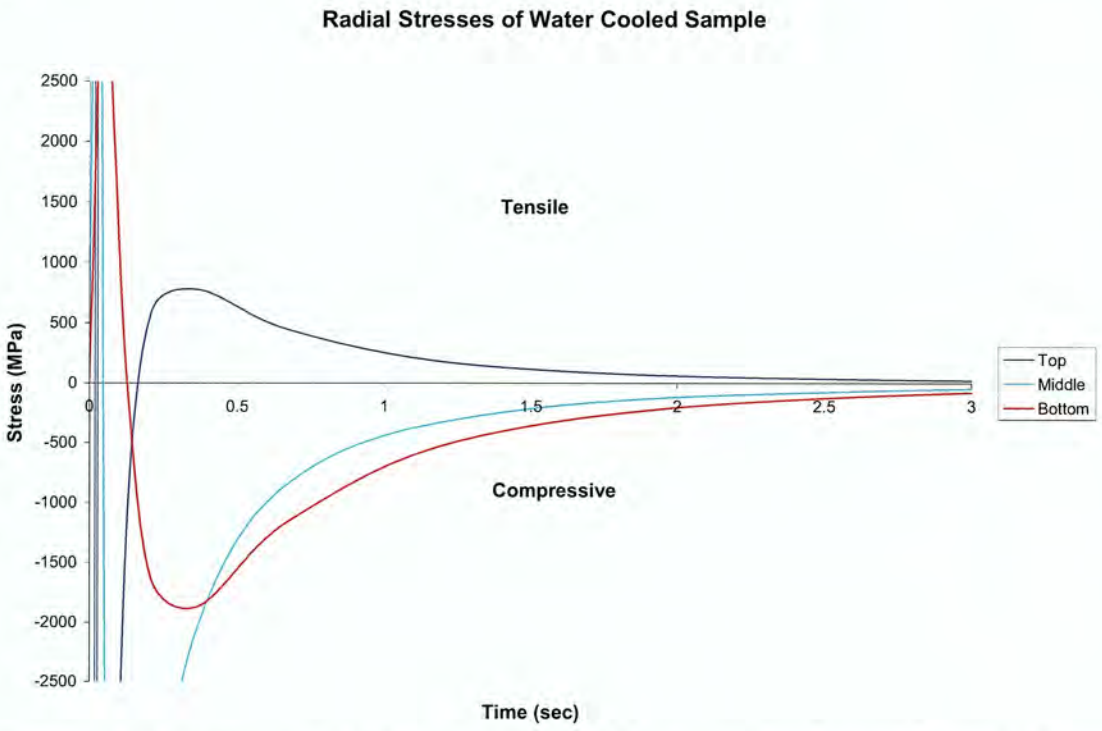


**Figure 9: Radial stresses at the top, middle and bottom of each sample graphed over time with the numerical model. a) Sample that is cooled with air. b) Sample that is cooled with water.**

## 3.6 Conclusions

Research demonstrated that controlled cracking due thermal shock phenomenon — where a part subjected to sudden temperature changes is prone to the formation of internal thermal stresses that may weaken the material to the extent of fracture— can be exploited for cutting brittle materials such as alumina. The process maps developed provide the regions of uncontrolled cracking, controlled cracking and scribing as a function of energy input into the sample. Water-assisted laser cutting showed distinct regions for the three sample fracture characteristics: scribing, controlled cracking and uncontrolled cracking. Controlled fracture of alumina during water-assisted laser cutting was correlated to threshold input energy

density and was observed at feed rates that are approximately 500% faster than previous reports on alumina machining. Process map of dry laser cutting do not demonstrate an interconnection between input energy density input and observed sample fracture characteristics. Thermo-elastic analysis indicated that sample surface is subjected to thermal shock phenomena during water-assisted laser cutting leading to build-up of tensile stresses in a small volume on the alumina surface. However during dry laser cutting, the slow cooling rate precludes the development of tensile stresses and most of the surface damage is induced due to melting and ablation of materials. Results of this study suggest that water-assisted laser machining is a feasible manufacturing process for cutting of alumina at lower laser powers and improved cutting speed than the traditional dry laser cutting while maintaining excellent surface integrity and tighter tolerances.

### 3.7 Acknowledgments

The authors gratefully acknowledge the financial support for this research provided by the U.S. National Science Foundation under the Grant DMI-0522788.

### 3.8 References

1) L.M. Sheppard, "Machining of advanced ceramics," Advanced Materials and Processes, ASM, 12, 40, 1987

2) B.E. Brath, "$CO_2$ laser cutting of ceramic tile", Beng. Dissertation, Heriot-Watt University,Edinburgh, UK, 1994.

3) G. Chryssolouris, "Laser Machining: Theory and Practice", Springer, Berlin, 1991.

4) M.U. Islam, "Laser machining of ceramics: a review," Materials and Manufacturing Processes", 8 (6), 611-630, 1993.

5) E. Dörre and H.Hübner, Alumina. Berlin: Spring-Verlag, 1984.

6) R. Codingley, R., Kohan, R.L., Ben-Nissan B. and Pezzotti G. "Alumina as an Orthopaedic Biomaterial – Characteristics, Properties, Performance and Applications", The Journal of the Australasian Ceramic Society, 39, 1, 20-28, 2003.

7) Synrad Inc. $CO_2$ Laser Applications. 6 Feb. 2006. Applications News Letter Issue 130. 15 Feb. 2006. <http://www.synrad.com/e-newsletters%5C02_02_06.htm>.

8) D.K. Patel and J.D. Baker, (1992), ''Method for Laser Scribing Substrates,'' U.S. patent No. 5,116,641.

9) C.H. Tsai and C.S. Liou, (2003), "Fracture Mechanism of Laser Cutting With Controlled Fracture." Journal of Manufacturing Science and Engineering, 125, p.519.

10) R.M. Lumley, (1969), "Controlled Separation of Brittle Materials Using a Laser,'' Am. Ceram. Soc. Bull., 48, p.850.

11) A.E. Segal, G. Cai, R. Akarapu, A. Romasco and B. Li, "Fracture control of unsupported ceramics during laser machining using a simultaneous prescore", Journal of Laser Applications, 17, 1, 57-62, 2005.

12) P. Santiago, M. Washington, P. Brugan, G. Cai, R. Akarapu, S. Pulford and A.E.Segall, "Faster and damage reduced laser cutting of thick ceramics using a simultaneous prescore approach", Journal of Laser Applications, 2005.

13) C. Barnes, P. Shrotriya and P. Molian, "A hybrid laser/water-jet cutting process for brittle materials", 31st NAMRC Conference, Marquette University, May 23- 26, 2006.

14) R. Akarapu, B. Li, and A.E. Segall, A.E., "A thermal stress failure model for laser cutting and forming operations", Journal of Failure Analysis and Prevention, 4, 51-62, 2004.

15) Accratus. Aluminum Oxide home page. 16 Jan.http://www.accuratus.com/alumox.html

16) N. Noda, R.B. Hetnarski, and Y. Tanigawa, Thermal Stresses, 2nd, Taylor and Francis, New York, 2003.

17) Accu-Tech. HomePage. 17. Feb. http://www.accutechlaser.com/acc_ladrill.html

18) R.D. Cook, D. S. Malkus, P. E. Michael, and R. J. Witt, "Concepts of Applications of Finite Element Analysis 4th", Wiley & Sons, Inc., 2002.

19) N. Noda, "Thermal Stresses in Functionally Graded Materials", 3rd International Congress on Thermal Stresses, Thermal Stresses 99', Cracow, Poland; June 13-17, 1999.

## 3.9 TABLES

### Table 1: Properties of 96% alumina

| Property | Units | SI/Metric | (Imperial) |
|---|---|---|---|
| Density | gm/cc ($lb/ft^3$) | 3.72 | 232.2 |
| Flexural Strength | MPa ($lb/in^2x10^3$) | 345 | 50 |
| Elastic Modulus | GPa ($lb/in^2x10^6$) | 300 | 43.5 |
| Tensile Strength | MPa ($lb/in^2x10^3$) | 220 | 17.4 |
| Shear Modulus | GPa ($lb/in^2x10^6$) | 124 | 18 |
| Bulk Modulus | GPa ($lb/in^2x10^6$) | 172 | 25 |
| Poisson's Ratio | — | 0.21 | 0.21 |
| Compressive Strength | MPa ($lb/in^2x10^3$) | 2100 | 304.5 |
| Hardness | $Kg/mm^2$ | 1100 | — |
| Fracture Toughness $K_{IC}$ | $MPa•m^{1/2}$ | 3.5 | — |
| Thermal Conductivity | W/m•°K (BTU•in/$ft^2$•hr•°F) | 25 | 174 |
| Coefficient of Thermal Expansion | $10^{-6}$/°C ($10^{-6}$/°F) | 8.2 | 4.6 |
| Specific Heat | J/Kg•°K (Btu/lb•°F) | 880 | 0.21 |

### Table 2: Test parameter grid

| Power (Watts) | Feedrates (mm/sec) | | | | | | | | | | |
|---|---|---|---|---|---|---|---|---|---|---|---|
| 100 | 42.3 | 50.8 | 59.3 | 67.7 | 76.2 | 84.7 | 93.1 | 101.6 | 110.1 | 118.5 | 127 |
| 150 | 42.3 | 50.8 | 59.3 | 67.7 | 76.2 | 84.7 | 93.1 | 101.6 | 110.1 | 118.5 | 127 |
| 200 | 42.3 | 50.8 | 59.3 | 67.7 | 76.2 | 84.7 | 93.1 | 101.6 | 110.1 | 118.5 | 127 |
| 250 | 42.3 | 50.8 | 59.3 | 67.7 | 76.2 | 84.7 | 93.1 | 101.6 | 110.1 | 118.5 | 127 |
| 300 | 42.3 | 50.8 | 59.3 | 67.7 | 76.2 | 84.7 | 93.1 | 101.6 | 110.1 | 118.5 | 127 |

# Chapter 4: Conclusions

## 4.1 General Conclusions

A hybrid laser/water-jet (LWJ) cutting using low pressure water was demonstrated as a thermal stress fracture technique for machining glass, silicon and concrete. Spider web cracks in glass, meridian cracks in silicon and channel cracks in concrete were able to cleanly separate the material along the moving path of the laser beam. In the present set-up, the energy efficiency benefits of the hybrid manufacturing were not realized, although the quality of machined cuts were improved as compared to conventional laser cutting. The probable material removal mechanism involves induction of compressive stresses during laser heating followed by a change of stress field from compression to tension during water-jet cooling, leading to the crack initiation and growth from the upper to lower surface. It is not clear what would be the state of stress at the crack tip and whether material removal occurs through a stable or unstable crack propagation mode. The LWJ has vast potential for machining a variety of brittle materials by offering benefits such as reduced energy, increased cutting speed, improved accuracy and finish, and controlled depth, shape and taper.

Research demonstrated that controlled cracking due thermal shock phenomenon —where a part subjected to sudden temperature changes is prone to the formation of internal thermal stresses that may weaken the material to the extent of fracture— can be exploited for cutting brittle materials such as alumina. The process maps developed provide the regions of uncontrolled cracking, controlled cracking and scribing as a function of energy input into the sample. Water-assisted laser cutting showed distinct regions for the three sample fracture

characteristics: scribing, controlled cracking and uncontrolled cracking. Controlled fracture of alumina during water-assisted laser cutting was correlated to threshold input energy density and was observed at feed rates that are approximately 500% faster than previous reports on alumina machining. Process map of dry laser cutting do not demonstrate an interconnection between input energy density input and observed sample fracture characteristics. Thermo-elastic analysis indicated that sample surface is subjected to thermal shock phenomena during water-assisted laser cutting leading to build-up of tensile stresses in a small volume on the alumina surface. However during dry laser cutting, the slow cooling rate precludes the development of tensile stresses and most of the surface damage is induced due to melting and ablation of materials. Results of this study suggest that water-assisted laser machining is a feasible manufacturing process for cutting of alumina at lower laser powers and improved cutting speed than the traditional dry laser cutting while maintaining excellent surface integrity and tighter tolerances.

### 4.2 Significant Findings

To the author's knowledge these studies are the first to experimentally test a hybrid laser/water-jet system to thermally fracture brittle materials. Furthermore, this study is the first to create criteria maps, based on laser power and feedrate, for the effects of cutting brittle materials, as well as, defining a specific energy density input for controlled cracking of alumina with the use of laser and water quenching.

### 4.3 Future Work

It is the hope of the author that the experimental results will lead to a comprehensive set of criteria and characteristics that will enable the process of using thermally induced fracturing to

become a viable way of processing brittle materials. At the current time data has been collected with the use of the laser and water system and a 2-D model has been developed to numerically find temperature gradients and stress contours through out the materials. Presently, a 3-D numerical model is being investigated; in the hopes of a better understanding of controlling thermally induced cracks in brittle materials. Also, future experiments will be performed using a laser and high pressure water-jet system; in which the forces of not only thermal gradients but water pressure can be tested and observed.

## Acknowledgements

The author would like to thank his co-major professors, Dr. Pal Molian and Dr. Pranav Shrotriya, and also his non-major program of study committee member Dr. Frank Peters for their guidance and tutelage. He would also like to thank his parents, Linda and Jerry Barnes as well as his fiancée Melanie Cole, for which without their support none of this could have been possible. The author would also like to gratefully acknowledge the financial support for this research provided by the U.S. National Science Foundation under the Grant DMI-0522788.